LIMNOLOGY and OCEANOGRAPHY

ASLO

Limnol. Oceanogr. 9999, 2022, 1–20

doi: 10.1002/lno.12098

Long-term change in metabolism phenology in north temperate lakes

Robert Ladwig,[1*] **Alison P. Appling**,[2] **Austin Delany**,[1] **Hilary A. Dugan**,[1] **Qiantong Gao**,[1] **Noah Lottig**,[3] **Jemma Stachelek**,[1] **Paul C. Hanson**[1]

[1]Center for Limnology, University of Wisconsin-Madison, Madison, Wisconsin
[2]U.S. Geological Survey, University Park, Pennsylvania
[3]Center for Limnology Trout Lake Station, University of Wisconsin-Madison, Boulder-Junction, Wisconsin

Abstract

The phenology of dissolved oxygen (DO) dynamics and metabolism in north temperate lakes offers a basis for comparing metabolic cycles over multi-year time scales. Although proximal control over lake DO can be attributed to metabolism and physical processes, how those processes evolve over decades largely remains unexplored. Metabolism phenology may reveal the importance of coherence among lakes and facilitate general conclusions about the controls on lake metabolism at regional scales. We developed a Bayesian modeling framework to estimate DO concentrations and metabolism in eight lakes in contrasting landscapes in Wisconsin, USA. We identify the DO and metabolism phenologies for each lake, and use those to compare how decadal patterns relate to trophic state and landscape setting. We show that lakes can be categorized by their hypolimnetic oxygen consumption dynamics, with oligotrophic lakes having a diverse set of patterns and eutrophic lakes having uniform trends of increased oxygen consumption over the last decade. Metabolism phenology is likewise diverse for oligotrophic lakes, whereas eutrophic lakes in southern Wisconsin share consistent long-term patterns of metabolic trends and seasonal DO consumption highlighting the importance of trophic state driving metabolism. Eutrophic lakes had higher magnitudes and more seasonal variation in net ecosystem production in contrast to oligotrophic lakes. Generally, long-term metabolic trends of north temperate lakes suggest a limited influence of climate on lake metabolism and that temporal coherence of long-term metabolism change is driven primarily by the landscape setting.

Lake phenology is well described for the seasonal emergence of biotic communities and their linkages to the annual physical dynamics of dimictic temperate lakes (Sommer et al. 2012). Phenology can be extended to lake dissolved oxygen (DO) dynamics as an integrator of the metabolic processes of primary production and respiration, which are responsive to the annual cycles in temperate lakes. As articulated by Edward A. Birge one century ago:

> […] [T]he cycle of the [oxygen] changes in a lake illustrates more readily and more conspicuously than perhaps any other facts could do what may be called the "annual life cycle" of the individual lake, showing both the underlying resemblances of that cycle as found in different lakes and also some small part of the infinite variation in its details. (Birge 1910)

Metabolism phenology provides a conceptual basis for comparing the annual metabolic cycles of lakes and how those cycles might evolve through time in response to both exogenous drivers, such as land use and climate change, and internal physical–chemical–biological interactions (Sommer et al. 2012). Both metabolism as an ecosystem process and dissolved oxygen (DO) as an ecosystem state variable have linkages to phenology. Water temperature, which has a strong annual signal, regulates gas solubility, as well as biological and geochemical reactions that produce or consume oxygen (Staehr et al. 2010). In many lakes, biological fluxes of oxygen production (photosynthesis) and consumption (respiration) dominate short-term changes in DO (Cole et al. 2000; Hanson et al. 2003; Solomon et al. 2013). Metabolic dynamics at the lake ecosystem scale are associated with a variety of processes

*Correspondence: rladwig2@wisc.edu

Additional Supporting Information may be found in the online version of this article.

Author Contribution Statement: R.L., P.C.H., and L.G. designed the study. L.G., A.D., and R.L. pre-processed the input data. P.C.H., L.G., N.L., and R.L. performed the lake model simulations. P.C.H., H.A.D., and R.L. analyzed the data. A.A. and J.S. made significant contributions to the verification and presentation of results. All authors contributed to the preparation of the manuscript and approved the final submitted manuscript.

and conditions that are seasonally dependent, such as autochthony and allochthony (Hanson et al. 2003; Tsai et al. 2008; Carey et al. 2018), light availability (Staehr et al. 2016; Phillips 2020), water temperature (Hanson et al. 2011; Scharfenberger et al. 2019), and phytoplankton dynamics (Kamarainen et al. 2009; Staehr et al. 2016). With climate and land use change, it is reasonable to hypothesize that DO and metabolism phenology in lakes are changing (Jenny et al. 2016; Woolway et al. 2021).

Climate change is known to affect the phenology of populations by creating stochastic mismatches between the timing of species life cycles and their environment (Yu et al. 2017; Liu et al. 2022). However, it is often unknown how long-term phenology and drivers observed in a single aquatic ecosystem relate to aquatic ecosystems found throughout a region. Searching for commonality in lake phenology has the potential to reveal the existence of coherence among lakes and facilitate more general conclusions about the controls on lake metabolism at regional scales. If coherent clusters among nearby lakes can be established, the conclusions drawn about lake metabolism may apply beyond the specific lakes under study (Magnuson et al. 1990). To begin, one needs long-term observational data, a DO and metabolism model that captures essential processes and includes distinct strata that have relevance to water quality and habitability, and a metabolism phenology modeling framework that accounts for the influence of ecosystem stochasticity and long-term change. Such a framework then provides quantified prediction of critical ecosystem patterns in observable variables, such as the response of DO to net ecosystem production (NEP) and the depletion of DO concentrations, that is,

$$\frac{d[\mathrm{DO}]}{dt} = \mathrm{GPP} - \mathrm{ER} + D = \mathrm{NEP} + D, \quad (1)$$

where GPP is gross primary production, ER is ecosystem respiration, and D is the exchange with the atmosphere (Odum 1956; van de Bogert et al. 2007; Hoellein et al. 2013).

Existing modeling approaches offer helpful insights as a plethora of aquatic ecosystem models (AEMs) has been developed (Mooij et al. 2010) to examine the impact of external or internal forcings on aquatic ecosystem states and processes (Janssen et al. 2015). AEMs usually consist of a hydrodynamic model coupled to a water quality/ecosystem model, with variable feedback loops between both models. Models can differ substantially in their respective approaches, that is, hydrodynamically they could apply an integral energy approach, that is, DYRESM (Dynamic Reservoir Simulation Model, Hamilton and Schladow 1997), GLM (General Lake Model, Hipsey et al. 2019) or MyLake (Multi-year Lake simulation Model, Saloranta and Andersen 2007), or quantify vertical changes of turbulent kinetic energy, that is, GOTM (General Ocean Turbulence Model, Burchard et al. 1999), LAKE2.0 (Stepanenko et al. 2016) or Simstrat (Goudsmit et al. 2002). State-of-the art vertical one-dimensional AEMs include GLM-AED (Hipsey et al. 2019), MyLake (Saloranta and Andersen 2007), WET (Nielsen et al. 2017), Simstrat-AED (Goudsmit et al. 2002), and PCLake (Janssen et al. 2019). The prediction realism that can be generated from AEMs has associated costs that challenge the application of these models across broad space and time scales or across populations of lakes. The high number of parameters create equifinality issues (Beven 2006), and high data and computational requirements, as well as requirements for end-user skill, can lead to lower flexibility and adaptability of such models to new kinds of problems (e.g., applying an advanced autocalibration routine as in Luo et al. 2018). Simpler models, designed specifically for aquatic metabolism, have been tailored toward reproducing diel DO dynamics from high-frequency sensor networks (Coloso et al. 2008; Holtgrieve et al. 2010; Sadro et al. 2011; Staehr et al. 2012*b*; Giling et al. 2017; Appling et al. 2018). Rarely, do these models incorporate hydrodynamics nor have they been applied at longer time scales, with a few exceptions (Solomon et al. 2013). Thus, neither AEMs nor diel metabolism models fit the problem of long-term metabolism phenology and a combination of these approaches is needed to address the challenge of modeling long-term metabolism phenology.

Our approach was to develop a physically and ecologically simplified model in which biological processes are not explicitly simulated, but integrated into a fitting parameter, which we dynamically estimated using field data in a Bayesian approach. Furthermore, although physically simplified, we mathematically approximated thermally stratified lakes as two-layer systems, in which an idealized well-mixed surface volume (i.e., the epilimnion) is separated by an area with a sharp density gradient (i.e., the thermocline) from a well-mixed bottom volume (i.e., the hypolimnion). The two-layer assumption is applied because of our focus on long-term dynamics neglecting well-known fluid dynamic processes (e.g., internal waves, density currents, convective overturn, *see* Bouffard and Wüest 2019; Imberger and Hamblin 1982). Nonetheless, we assume that both volumes exhibit DO and metabolism dynamics that are—to a certain extent—independent from each other and that the metabolic fluxes can be applied to each layer separately. Such a two-layer DO model for lakes that accounts for dynamic shifts between mixed conditions in the fall to spring to stratified conditions in the summer builds a more holistic and comprehensive representation of pelagic DO concentrations and metabolic fluxes, and—although simplified—can be used for the quantification of long-term changes of pelagic DO and metabolism. An important caveat is that spatial heterogeneity in DO can be high (van de Bogert et al. 2007) due to spatial variability in metabolism (Brothers and Vadeboncoeur 2021) and the influence of mixing and lateral flow on observed DO patterns (MacIntyre and Melack 1995; Staehr et al. 2010).

We use this approach to quantify the metabolic dynamics of eight dimictic north temperate lakes in Wisconsin and

Table 1. Characteristics of lakes in this study, including depth (maximum/mean), RT, mean total nitrogen (TN) and mean total phosphorus (TP). DO data provide the number of DO profiles (summer: April to November/total) since monitoring began. RT is not calculated for Fish Lake since it is a closed-basin system.

	Lake	Area (ha)	Depth (m)	RT (yr)	Mean TN (μg L^{-1})*	Mean TP (μg L^{-1})*	Secchi depth (m)†	DO data*
North	Allequash	164.2	8/2.9	0.5‡	281	14	3.3	568/673 since 1981
	Big Muskellunge	363.4	21.3/7.5	8‡	277	7	7.0	573/675 since 1981
	Crystal	37.5	20.4/10.4	12.7‡	139	4	7.6	598/701 since 1981
	Sparkling	63.7	20/10.9	10.4‡	188	5	6.2	573/677 since 1981
	Trout	1565.1	35.7/14.6	4.6‡	182	5	5.3	576/676 since 1981
South	Fish	80.4	18.9/6.6	NA	749	18	NA	315/348 since 1996
	Mendota	3961.2	25.3/12.8	4.3§	954	50	1.8	363/406 since 1995
	Monona	1359.8	22.5/8.2	0.7§	816	47	3.0	341/375 since 1995

*Magnuson et al. (2020*a*, 2006).
†Magnuson et al. (2021*a*).
‡Webster et al. (1996).
§Lathrop and Carpenter (2014).

study their long-term metabolism phenology. We use a Bayesian Markov Chain Monte Carlo approach to fit metabolism model parameters for NEP in the epilimnion and the hypolimnion, and a parameter for the sediment oxygen demand. The simplicity and data-intensive nature of the approach allows the model to be applicable to a wide range of potential lake ecosystems without relying on an over-parameterized mathematical approach. Using the output of the model, we characterize DO and metabolic phenology and address the questions: How do major physical and metabolic DO fluxes compare among lakes in the two different landscape settings? Has the phenology of metabolism in these lakes changed over several decades, and is there a temporal coherence of NEP to the landscape setting or to climate?

Methods

Study sites

Eight lakes of the North Temperate Lakes Long-Term Ecological Research program (NTL-LTER[1]; Magnuson et al. 2006) were included in this study. Five of the lakes (Allequash, Big Muskellunge, Crystal, Sparkling, and Trout) are situated in the Northern Highland Lake District in northern Wisconsin in a mixed pine/hardwood forest and have been monitored since 1981 (Carpenter et al. 2007). Big Muskellunge, Crystal, and Sparkling Lakes are groundwater seepage lakes with residence times (RTs) >8 years (Table 1), whereas Allequash and Trout Lakes are drainage lakes (Webster et al. 1996). In southern Wisconsin, three lakes (Fish, Mendota, and Monona), are in predominantly agricultural and urban watersheds (Carpenter et al. 2007; Magee and Wu 2017*a*) and have been monitored by the NTL-LTER since 1995. The northern lakes are oligotrophic, except for mesotrophic Allequash (Table 1). The southern lakes are predominantly eutrophic, except for Fish that shifts between mesotrophic or eutrophic, and all the southern lakes experience prolonged anoxia every summer. The eight lakes span a range in size, depth, RT, and trophic status, and are representative of north temperate dimictic lakes embedded in glacial deposits (Table 1).

Modeling framework

Our goals were to calculate decadal changes in both epilimnetic and hypolimnetic DO by quantifying dominant metabolic and physical fluxes and evaluate long-term metabolic phenology. We have constructed a framework that emphasizes seasonal dynamics and that captures important seasonal transitions, such as spring and fall mixing, the development of summer stratification, and winter ice cover (although simplified). Our framework accounts for long-term change in ecosystem-scale metabolic fluxes and quantifies associated uncertainties. As DO dynamics are strongly associated with the cyclicity and seasonality of aquatic metabolism, our framework addresses long-term changes in the phenology of metabolic fluxes and dynamics in the eight lakes. All the lakes stratify during the summer months and to a certain extent fulfill the vertical one-dimensional model assumption, meaning that their density gradient over the vertical axis is larger than over the horizontal axis. Thus, we simplified their long-term dynamics using a two-layer model with the focus on modeling vertical transport processes. For a discussion of our use of the vertical one-dimensional model assumption for these lakes, *see* Supporting Information, "Checking the vertical one-dimensional model assumption." Our model has the following main assumptions: (a) a lake is either stratified with two fully mixed volumes or mixed in one total volume, (b) while lakes are ice-covered, we assume mixed conditions and minimal air-water interactions, and (c) fitting a small number of

[1]lter.limnology.wisc.edu

parameters (dynamically through time) enables us to discriminate the metabolic and physical processes controlling DO observed from field data and study how those processes change through time.

Our modeling framework links several models (a hydrodynamic lake model, a process-based metabolism model, and a statistical model) to form a process-error modeling framework (Fig. 1) that weighs the information in observational data to account for the uncertainty in the process-based model. For each lake, we constructed time series of epilimnion and hypolimnion temperatures and volumes, and thermocline depths from outputs of a hydrodynamic lake model. These variables were subsequently used in a process-based metabolism model to simulate DO concentrations and the respective fluxes. Using a Bayesian framework, we created posterior estimates for three parameters in the metabolism model when observational data were available. Simulations for each lake were run from 1979 to 2019. We analyzed the model outputs using time-series decomposition to identify trend and seasonal components and used clustering of time-series data to inspect coherence between sites and across time. A detailed description of each of these steps is provided below.

Process-based metabolism model

The lake water column was categorized as stratified (during summer conditions, with a vertical density difference between surface and bottom layer that exceeded 0.05 kg m^{-3}, an average water temperature above 4°C, and presence of a thermocline) or completely mixed (Fig. 1, upper left corner). During stratified conditions, we approximated the vertical layering of the water column into two completely mixed volumes: the epilimnion and the hypolimnion. Both layers were separated by an idealized zone of low vertical diffusivity (the thermocline), which acted as a barrier to transport. The thermocline is part of a wider zone, the metalimnion. For simplicity, we partitioned the metalimnion to either the epilimnion or the hypolimnion depending on the depth of the thermocline. Our model neglects the existence of an inverse stratification period during ice-covered winter periods, and assumes completely mixed water column conditions. We did not model under ice conditions due to our focus on long-term metabolism dynamics during summer stratified conditions and due to a lack of long-term under ice DO data, although aquatic ecosystems are affected by under-ice interactions between the abiotic and biotic environment (Jansen et al. 2021).

Our metabolism model approximated the general ordinary differential DO equation of each layer as a discrete first-order linear forward differencing solution using an explicit forward Euler scheme and a daily time step:

$$\frac{d[\mathrm{DO}]}{dt} = \sum_{a}^{n} F_a, \qquad (2)$$

$$[\mathrm{DO}]_{t+1} = \left([\mathrm{DO}]_t + \sum\nolimits_a^n F_{a,t} * \Delta \mathrm{t}\right) * \frac{V_t}{V_{t+1}},$$

where [DO] is the DO concentration (mg m^{-3}), F represents the a^{th} flux over n total fluxes that either increase or decrease DO (mg m^{-3} d^{-1}), Δt is the time step, and V (m^3) is the volume. The volume conversions are included as our DO state variables are in concentration units and the specific volumes of epilimnion and hypolimnion are dynamic over time. The metabolism model was coded in Stan (Stan Development Team 2019), using the rstan-package (Stan Development Team 2020).

When the lake water column was under mixed conditions, the model calculated total DO concentration as a function of direct atmospheric exchange (F^{ATM}, mg m^{-3} d^{-1}), NEP ($F^{\mathrm{NEP,epi}}$, mg m^{-3} d^{-1} as well as $F^{\mathrm{NEP,hypo}}$, mg m^{-3} d^{-1}), and mineralization through sediment oxygen demand (F^{SED}, mg m^{-3} d^{-1}):

$$[\mathrm{DO}]_{t+1}^{\mathrm{total}} = \begin{cases} \left([\mathrm{DO}]_t^{\mathrm{epi}} * V_t^{\mathrm{epi}} + [DO]_t^{\mathrm{hypo}} * V_t^{\mathrm{hypo}}\right) * V_{t+1}^{\mathrm{total}\,-1}, & \text{if stratified,} \\ \left([DO]_t^{\mathrm{total}} + \left(F_t^{\mathrm{ATM}} + F_t^{\mathrm{NEP,epi}} + F_t^{\mathrm{NEP,hypo}} - F_t^{\mathrm{SED}}\right) * \Delta t\right) * \dfrac{V_t^{\mathrm{total}}}{V_{t+1}^{\mathrm{total}}}, & \text{otherwise,} \end{cases} \qquad (3)$$

where $[\mathrm{DO}]_t^{\mathrm{total/epi/hypo}}$ is the DO concentration in the total, epilimnion, or hypolimnion layer, respectively, at time step t, and $V_t^{\mathrm{total/epi/hypo}}$ is the water volume in the total, epilimnion, or hypolimnion layer (m^3), respectively, at time step t.

During stratified conditions, the change of DO concentrations over time in the epilimnion is governed by a direct exchange with the atmosphere (F^{ATM}, mg m^{-3} d^{-1}), NEP ($F^{\mathrm{NEP,epi}}$, mg m^{-3} d^{-1}), DO entrainment from or into the hypolimnion by turbulent flow ($F^{\mathrm{ENTR,epi}}$, mg m^{-3} d^{-1}), and a diffusive DO flux between hypolimnion and epilimnion ($F^{\mathrm{DIFF,epi}}$, mg m^{-3} d^{-1}):

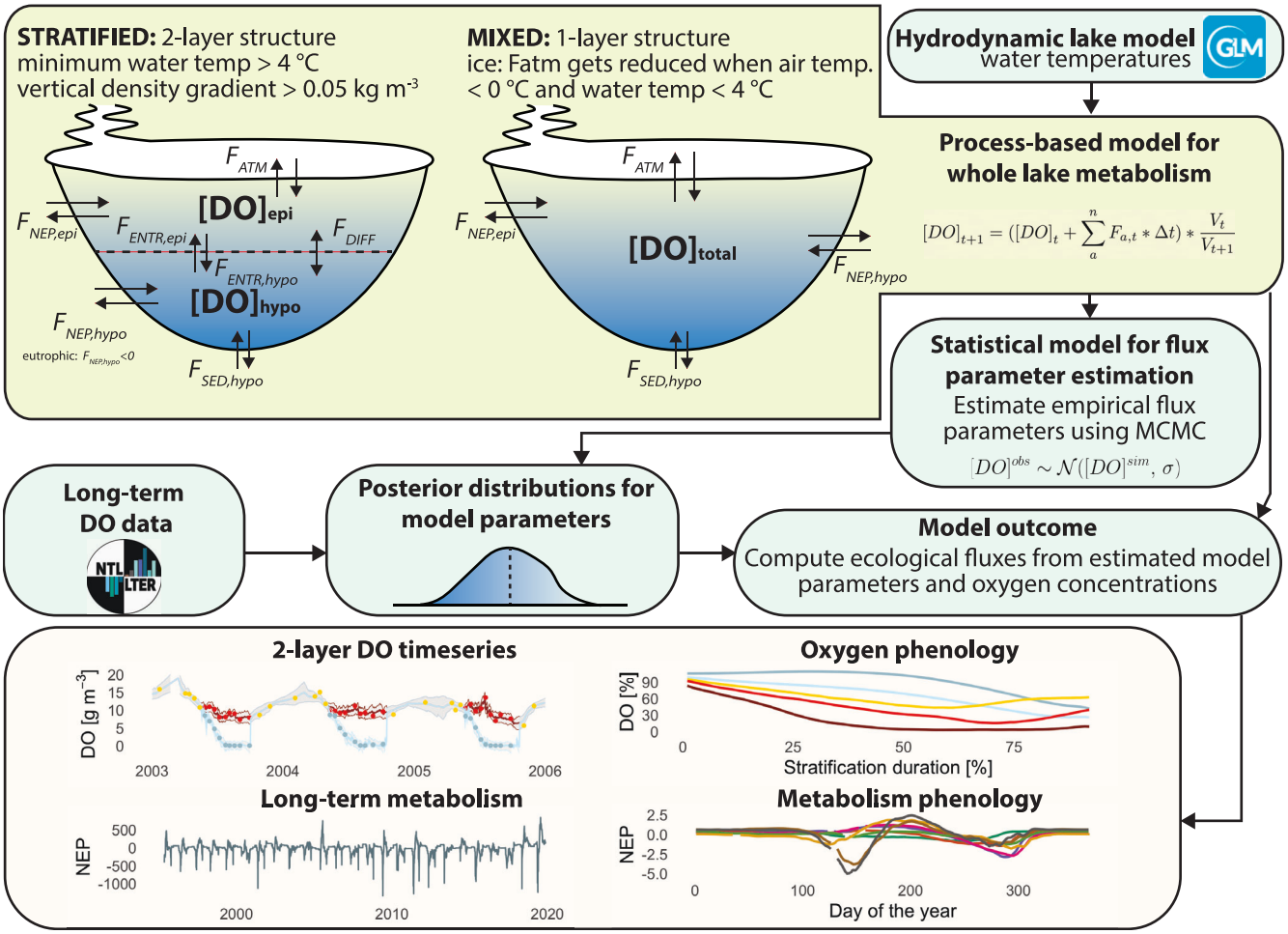

Fig. 1. Conceptual diagram illustrating our modeling workflow as outlined in the methods. The outputs of a hydrodynamic lake model (GLM), calibrated to each study site, were used to run a two-layer metabolism model. The free model parameters of the metabolism model were estimated using a Bayesian framework running multiple Markov chains. For this parameter estimation, long-term monitoring data of observed DO data were used to estimate the likelihood of the simulated oxygen data. Simulated oxygen time series and metabolism fluxes were analyzed to derive general information about long-term changes of metabolism phenology.

$$[\mathrm{DO}]_{t+1}^{\mathrm{epi}} = \begin{cases} \left([\mathrm{DO}]_t^{\mathrm{epi}} + \left(F_t^{\mathrm{ATM}} + F_t^{\mathrm{NEP,epi}} \pm F_t^{\mathrm{ENTR,epi}} \pm F_t^{\mathrm{DIFF,epi}}\right) * \Delta t\right) * \dfrac{V_t^{\mathrm{epi}}}{V_{t+1}^{\mathrm{epi}}}, & \text{if stratified,} \\ [\mathrm{DO}]_{t+1}^{\mathrm{total}}, & \text{otherwise.} \end{cases} \quad (4)$$

The same numerical metabolism scheme applies to the hypolimnion, where during stratified conditions the sources and sinks to DO concentrations over time in the hypolimnion are NEP ($F^{\mathrm{NEP,hypo}}$, mg m^{-3} d^{-1}), mineralization through sediment oxygen demand (F^{SED}, mg m^{-3} d^{-1}), DO entrainment into or from the epilimnion by turbulent flow ($F^{\mathrm{ENTR,hypo}}$, mg m^{-3} d^{-1}), and a diffusive DO flux between epilimnion and hypolimnion ($F^{\mathrm{DIFF,hypo}}$, mg m^{-3} d^{-1}):

$$[\mathrm{DO}]_{t+1}^{\mathrm{hypo}} = \begin{cases} \left([\mathrm{DO}]_t^{\mathrm{hypo}} + \left(F_t^{\mathrm{NEP,hypo}} - F_t^{\mathrm{SED}} \pm F_t^{\mathrm{ENTR,hypo}} \pm F_t^{\mathrm{DIFF,hypo}}\right) * \Delta t\right) * \dfrac{V_t^{\mathrm{hypo}}}{V_{t+1}^{\mathrm{hypo}}}, & \text{if stratified,} \\ [\mathrm{DO}]_{t+1}^{\mathrm{total}}, & \text{otherwise.} \end{cases} \quad (5)$$

Atmospheric DO exchange, F^{ATM} was modeled as:

$$F_t^{ATM} = \begin{cases} \dfrac{k_{t-1}^{epi}\left([DO]_{t-1}^{sat,epi} - [DO]_{t-1}^{epi}\right)}{z_{t-1}^{epi}}, & \text{if stratified,} \\ \dfrac{k_{t-1}^{total}\left([DO]_{t-1}^{sat,total} - [DO]_{t-1}^{total}\right)}{z_{t-1}^{mean}}, & \text{otherwise,} \end{cases} \quad (6)$$

where k is the gas transfer velocity after the method of Vachon and Prairie (2013) (m d^{-1}) dependent on lake area and observed wind speed, $[DO]^{sat}$ is the saturation DO concentration (mg m^{-3}) dependent on water temperature T (either in the epilimnion during stratified conditions, or otherwise in the total water column) and lake altitude (Garcia and Gordon 1992), t is the respective time step, and z refers to the thickness of the layer (m). In the stratified case, z equals the epilimnion thickness up to the thermocline depth while during mixed conditions z equals the mean lake depth. We used Lake Metabolizer for the atmospheric DO exchange calculations (Winslow et al. 2016). The estimation after Vachon and Prairie (2013) relates the gas transfer velocity to wind velocity and lake area, and sufficiently accounts for seasonal changes in atmosphere-water gas flux interactions as wind is expected to be the dominant driver of gas exchange in lakes larger than 100 ha (five of our eight lakes are larger than 100 ha, the others are only slightly smaller). Alternative methods consider additional variables and processes to account for processes other than wind-induced mixing like convective overturn (MacIntyre et al. 2010, 2021; Read et al. 2012; Heiskanen et al. 2014; Dugan et al. 2016), but as our modeling time step of 24 h neglects diurnal cycles, these methods were out of scope for our long-term study. To represent much reduced atmospheric exchange under ice conditions, we set k to 10^{-5} m d^{-1} when the lake was mixed, the air temperatures were below 0°C, and water temperatures were below 4°C. Gas transfer velocities are significantly reduced under ice cover (Butterworth and Miller 2016; Manning et al. 2019), with measured velocities close to $\sim 5\ 10^{-4}$ m d^{-1} (Lovely et al. 2015). As our focus is open-water conditions (in line with our observational data), we arbitrarily reduced air–water interactions during ice conditions and let the free fitting parameter determine the uncertainty of the metabolic fluxes.

The NEP flux, F^{NEP}, is the difference between GPP and ER, and depends on a free parameter, X, as well as a temperature coefficient. Therefore, NEP can either be a source or a sink term:

$$F_t^{NEP,epi} = \begin{cases} X_t^{NEP,epi} * \theta^{T_{t-1}^{epi}-20}, & \text{if stratified,} \\ X_t^{NEP,epi} * \theta^{T_{t-1}^{total}-20}, & \text{otherwise,} \end{cases} \quad (7)$$

and

$$F_t^{NEP,hypo} = \begin{cases} X_t^{NEP,hypo} * \theta^{T_{t-1}^{hypo}-20}, & \text{if stratified,} \\ X_t^{NEP,hypo} * \theta^{T_{t-1}^{total}-20}, & \text{otherwise,} \end{cases} \quad (8)$$

where the term depends on a parameter X^{NEP} (mg m^{-3} d^{-1}) which is the idealized NEP rate per unit time at a water temperature of 20°C, and θ, which is an Arrhenius multiplier set to 1.08 (included to make the fluxes dependent on water temperature), $T_t^{total/epi/hypo}$ is the water temperature (°C) in the total water column, epilimnion or hypolimnion layer, respectively, at time step t. For the eutrophic southern lakes, we set $F_t^{NEP,hypo}$ to only negative values as we assume that these lakes have no primary production below the thermocline, due to their high light extinction (Table 1, as the average Secchi depth is less than the mean depth as well as the eutrophic lakes having average euphotic zone depths above their mean as well as thermocline depths). We are referring to F^{NEP} as a flux throughout the manuscript, although it is mechanistically a source/sink term for DO. We are applying this simplification to consider all sources and sinks that affect DO in the metabolism model as fluxes, regardless if a transport process is involved or not.

The sediment flux, F^{SED}, is a sink in the metabolism model to represent sediment oxygen demand in the hypolimnion. The sediment flux followed a zero-order reaction scheme with a dynamic areal flux rate (representing the sediment oxygen demand) and a first-order reaction that depends on DO as well as the diffusive rate through a sediment boundary layer (Müller et al. 2012; Steinsberger et al. 2020). Similar to Steinsberger et al. (2020), this combined sediment flux includes the sum of a flux of reduced compounds from the sediment and the sediment oxygen uptake. In combination with the hypolimnetic NEP flux, $F_t^{NEP,hypo}$, which represents the water column mineralization if negative, both terms, $F_t^{SED} + F_t^{NEP,hypo}$, constitute the areal hypolimnetic mineralization. For simplification, F^{SED} is also used for quantifying $[DO]^{total}$ during mixed conditions:

$$F_t^{SED} = \begin{cases} \left(X_t^{SED} + \dfrac{D_{diff}}{\delta}[DO]_{t-1}^{hypo}\right) * \dfrac{A_{t-1}^{therm}}{V_{t-1}^{hypo}} * \theta^{T_{t-1}^{hypo}-20}, & \text{if stratified,} \\ \left(X_t^{SED} + \dfrac{D_{diff}}{\delta}[DO]_{t-1}^{total}\right) * \dfrac{A_{t-1}^{surf}}{V_{t-1}^{total}} * \theta^{T_{t-1}^{total}-20}, & \text{otherwise,} \end{cases} \quad (9)$$

where X^{SED} is the idealized areal flux rate per time unit (mg m^{-2} d^{-1}) at a water temperature of 20°C, D_{diff} is the molecular oxygen diffusion coefficient (m^2 s^{-1}), δ is the thickness of the diffusive boundary layer (m), and A is the respective area (m^2), either surface or thermocline area (Müller et al. 2012). We estimated the molecular diffusion coefficient of oxygen, D_{diff}, as a function of water temperature using the formula of Han and Bartels (1996):

$$\log_{10}(D_{\text{diff}}) = -4.410 + \frac{773.8}{T_{t-1}^{\text{hypo}} + 273.15} - \left(\frac{506.4}{T_{t-1}^{\text{hypo}} + 273.15}\right)^2, \quad (10)$$

where D_{diff} is in $\text{cm}^2\ \text{s}^{-1}$, and T_{t-1}^{hypo} is in °C.

The thickness of the diffusive boundary layer was assumed to be constant across all lakes with a value of 0.001 m, which is in the range of diffusive boundary layer thicknesses, 0.0002 to >0.001 m, according to Jørgensen and Revsbech (1985).

Entrainment fluxes, $F^{\text{ENTR,epi}}$ and $F^{\text{ENTR,hypo}}$, were included in the model to represent turbulent fluxes that either shallow or deepen the thermocline depth and therefore cause turbulent transport of DO into either the epilimnion or hypolimnion directly. These entrainment fluxes were only active during stratified two-layer conditions:

$$F_t^{\text{ENTR,epi}} = \begin{cases} \dfrac{V_{t+1}^{\text{epi}} - V_t^{\text{epi}}}{(t_{t+1} - t_t) * V_t^{\text{epi}}} * [\text{DO}]_t^{\text{hypo}}, & \text{if } V_{t+1}^{\text{epi}} \geq V_t^{\text{epi}} \\ \dfrac{V_{t+1}^{\text{epi}} - V_t^{\text{epi}}}{(t_{t+1} - t_t) * V_t^{\text{epi}}} * [\text{DO}]_t^{\text{epi}}, & \text{if } V_{t+1}^{\text{epi}} < V_t^{\text{epi}} \end{cases} \quad (11)$$

and

$$F_t^{\text{ENTR,hypo}} = \begin{cases} \dfrac{V_{t+1}^{\text{hypo}} - V_t^{\text{hypo}}}{(t_{t+1} - t_t) * V_t^{\text{hypo}}} * [\text{DO}]_t^{\text{epi}}, & \text{if } V_{t+1}^{\text{hypo}} \geq V_t^{\text{hypo}} \\ \dfrac{V_{t+1}^{\text{hypo}} - V_t^{\text{hypo}}}{(t_{t+1} - t_t) * V_t^{\text{hypo}}} * [\text{DO}]_t^{\text{hypo}}, & \text{if } V_{t+1}^{\text{hypo}} < V_t^{\text{hypo}}, \end{cases} \quad (12)$$

where both fluxes transport equal mass from or into the other respective layer.

Turbulent diffusive exchanges, F^{DIFF} ($\text{mg}\ \text{m}^{-3}\ \text{d}^{-1}$), were included in the model during stratified conditions to represent a turbulent diffusive exchange between the epilimnion and hypolimnion when entrainment fluxes are not occurring (hence, no fluctuations of the thermocline depth):

$$F_t^{\text{DIFF,epi}} = \frac{K_{t-1}}{A_{t-1}^{\text{therm}}}\left([\text{DO}]_{t-1}^{\text{hypo}} - [\text{DO}]_{t-1}^{\text{epi}}\right) \quad (13)$$

and

$$F_t^{\text{DIFF,hypo}} = \frac{K_{t-1}}{A_{t-1}^{\text{therm}}}\left([\text{DO}]_{t-1}^{\text{epi}} - [\text{DO}]_{t-1}^{\text{hypo}}\right). \quad (14)$$

The vertical turbulent diffusion coefficient, K $\left(\text{m}^2\,\text{d}^{-1}\right)$, between the epilimnion and hypolimnion was estimated using the approach by Hondzo and Stefan (1993) as

$$K = \alpha_k (N^2)^{-0.43}, \quad (15)$$

where α_k is a fitted parameter incorporating the lake surface area, and N is the buoyancy frequency (s^{-1}). We applied the empirical relationship from Hondzo and Stefan (1993) to calculate $\alpha_k = 0.00706\left(A^{\text{surf}}\right)^{0.56}$. The squared buoyancy frequency was quantified as

$$N^2 = \frac{g\partial\rho}{\rho\partial z}, \quad (16)$$

where g is gravitational acceleration ($\text{m}\ \text{s}^{-2}$), and ρ is water density ($\text{kg}\ \text{m}^{-3}$). We simplified this assumption by comparing the density differences between the epilimnion and the hypolimnion. Furthermore, we set all values of $N^2 < 7.0\,10^{-5}\ \text{s}^{-2}$ to $N^2 = 7.0\,10^{-5}\ \text{s}^{-2}$ (Hondzo and Stefan 1993). The approach relates the vertical turbulent diffusion coefficient to the lake area and buoyancy frequency, and was developed by Hondzo and Stefan (1993) for lakes in Minnesota, USA. As the diffusive transport of oxygen over the metalimnion is small compared to long-term DO dynamics driven by NEP or ecosystem respiration, we used this simplified estimation of vertical diffusion compared to most hydrodynamic models that either estimate eddy diffusivity by relating turbulent kinetic energy production to energy dissipation (e.g., Prandtl-Kolmogorov relationship as in Goudsmit et al. 2002) or by relating turbulent kinetic energy dissipation to the buoyancy frequency (e.g., as in the Weinstöck approach used in Hipsey et al. 2019).

Driver and field data

DO and temperature were recorded at the deepest location in each lake, from the surface to within 1 m of the bottom using a YSI Model 58 (pre-2011) or a YSI Pro-ODO (since 2011) (Magnuson et al. 2006, 2020*a*). Profiles were taken biweekly during the open water season, and 1–2 times when lakes were ice-covered. Our process-based metabolism model required evenly spaced monitoring data (e.g., daily data) of the vertical water temperature profile to calculate the following: thermocline depth, volume-averaged water temperatures of the epilimnion, hypolimnion and total volume, and the respective volumes of layers. Daily water temperature and wind speed were needed to calculate the atmospheric exchange of oxygen. We used simulated daily water temperatures generated by the General Lake Model (GLM v.2.2, Hipsey et al. 2019). GLM outputs for the lakes were obtained from Read et al. (2021), each calibrated from observed water temperature data (Read et al. 2019). For more information, *see* Supporting Information "GLM calibration". All GLM simulations neglected inflows and outflows. The thermocline depth was calculated as the depth of the center of buoyancy using the rLakeAnalyzer R package (Read et al. 2011). The respective average water temperatures, volumes of each layer, and the area at the thermocline were quantified using lake-specific hypsography (Magnuson et al. 2013, 2021*b*).

To calculate the daily atmospheric oxygen exchanges, we used daily-aggregated air temperature (to determine ice

conditions) and wind speeds from the second phase of the North American Land Data Assimilation System (Xia et al. 2012) with 1/8th-degree spaced grid cells centered at the specific lakes. Observed long-term DO concentrations for the estimation of the model parameters were obtained from NTL-LTER (Magnuson et al. 2020*a*). Layer-specific DO concentrations for the epilimnion and hypolimnion were calculated using volume-weighted averaging and the respective approximated thermocline depths. Fits of simulated DO to observed DO concentrations were quantified using the mean average error (MAE), the root-mean squared error (RMSE), the Nash–Sutcliffe coefficient of efficiency (NSE), and the regression coefficient (R^2).

Parameter estimation through inverse Bayesian modeling

We estimated three free model parameters $X^{NEP,epi}$, $X^{NEP,hypo}$, and X^{SED} using the general-purpose Bayesian modeling framework, Stan (Stan Development Team 2019), and the rstan (Stan Development Team 2020) interface to connect R to the Stan scripting language. The free flux parameters represent background ecosystem-scale processes and incorporate multiple ecological and biogeochemical processes. Applying a Bayesian framework for estimating the free metabolism parameters allowed the quantification of uncertainty, which is high due to multiple factors affecting in-lake ecosystem processes and the resulting uncertainties over the decadal scale. The X parameters were estimated whenever a mixing state

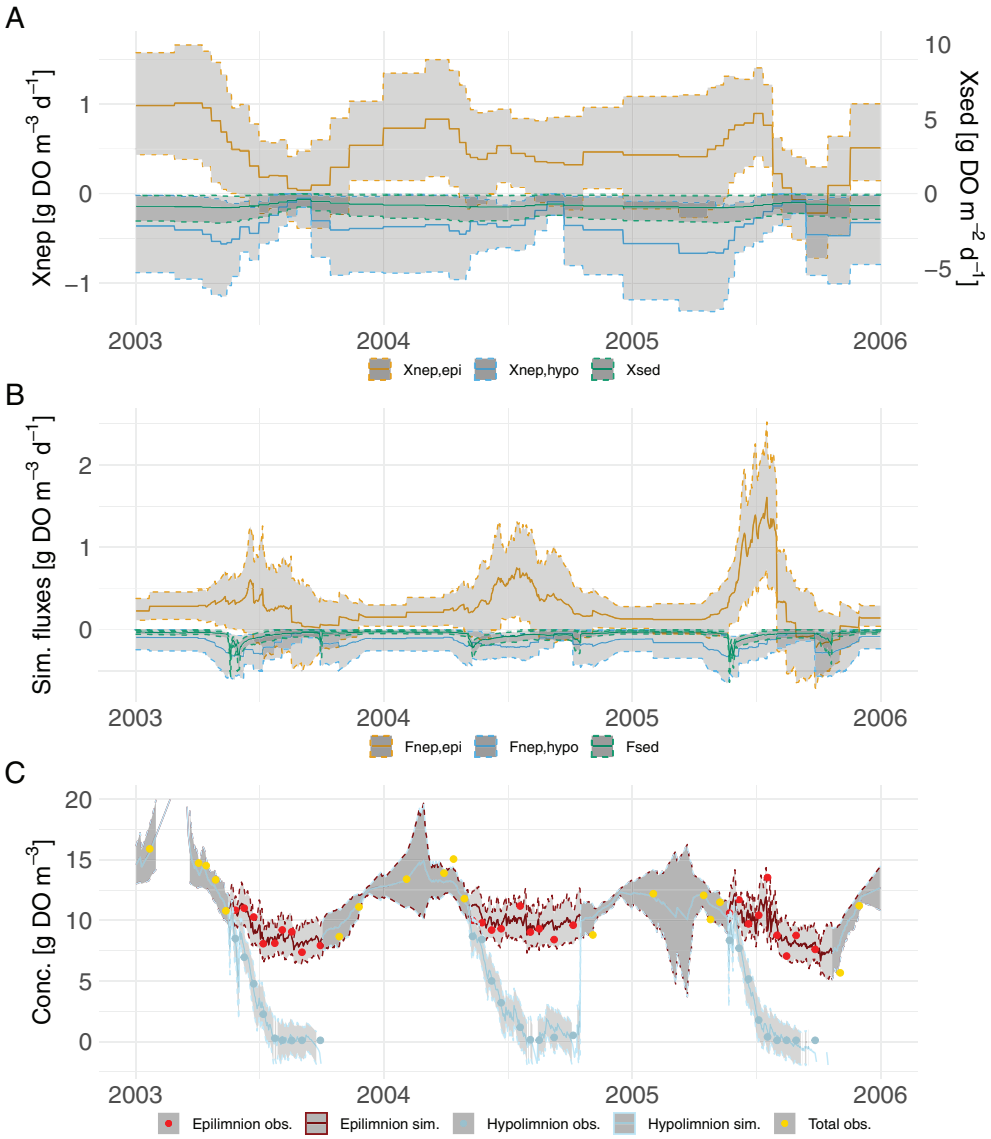

Fig. 2. Model results of Lake Mendota from 2003 to 2006. (**A**) Daily empirical flux parameters, which were estimated whenever a system shift from mixed to stratified, or vice versa, and when observed DO data were available. (**B**) Daily metabolism fluxes for NEP (in the epilimnion and hypolimnion) and sediment oxygen demand that were calculated using the estimated empirical flux parameters. (**C**) Simulated daily oxygen concentrations that were derived from the simulated metabolism fluxes in an explicit way. The gray bands of uncertainty represent the 97.5% and 2.5% quantiles.

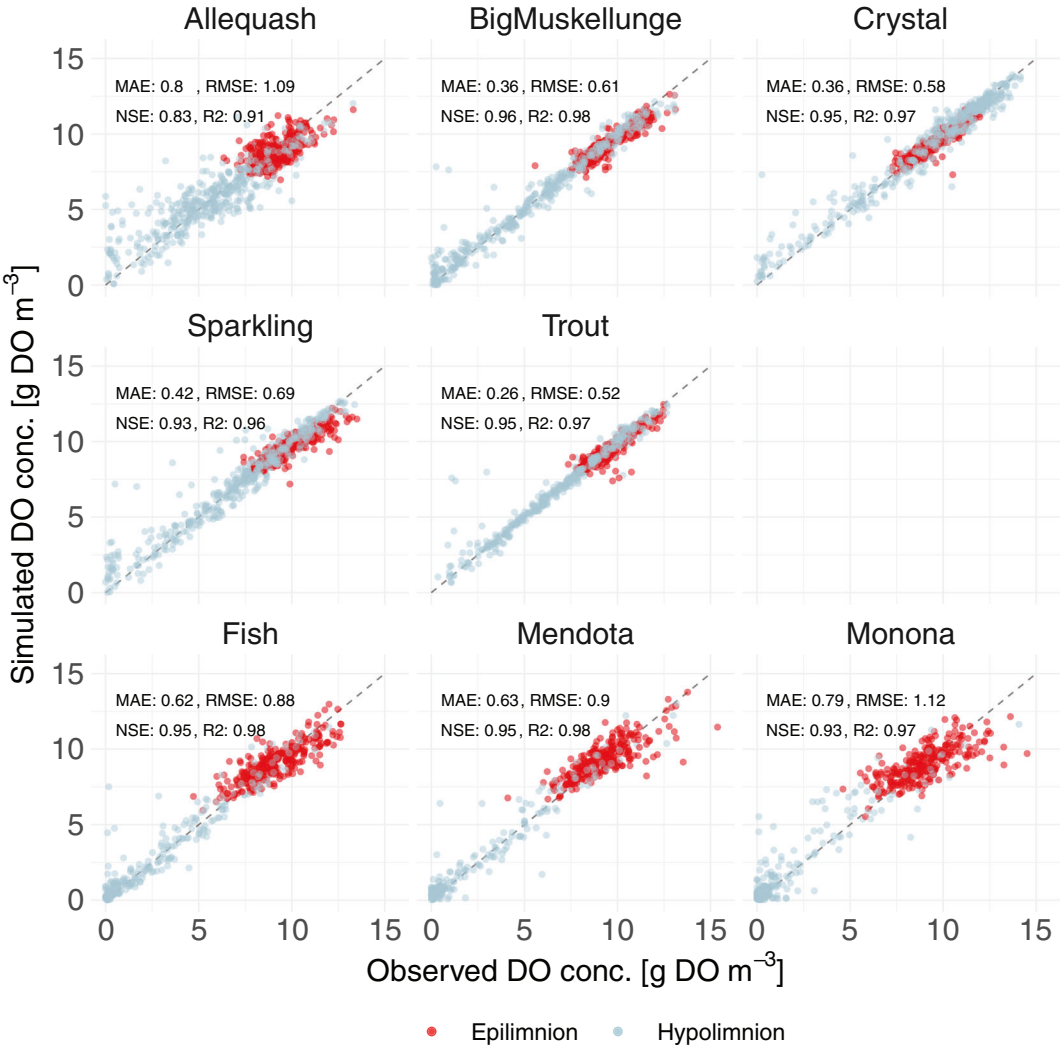

Fig. 3. Comparison between observed and simulated DO data for the eight lakes. Model fit is stated as MAE, RMSE, NSE, and regression coefficient (R^2). Red dots represent DO concentrations in the epilimnion (which includes stratified and nonstratified data) and blue dots represent concentrations in the hypolimnion. Dashed lines represent 1 : 1 lines to highlight the fit of observed to simulated data.

shift occurred (mixed to stratified conditions or vice versa) and whenever observed DO data were available, which resulted in most parameter estimations during the ice-free season. As we estimated free parameters for two fluxes acting simultaneously in the hypolimnion, we compared our estimates with alternative approaches to validate the modeling approach (*see* Supporting Information "Comparison of estimated hypolimnetic metabolic fluxes with alternative approaches"). For more information about the inverse Bayesian modeling framework, *see* Supporting Information "Bayesian modeling."

Time-series analysis

We decomposed the time series of all fluxes, $F^{\mathrm{NEP,epi}}$, $F^{\mathrm{NEP,hypo}}$, F^{SED} and $F^{\mathrm{NEP}}_{\mathrm{total}}$ ($F^{\mathrm{NEP}}_{\mathrm{total}} = F^{\mathrm{NEP,epi}} + F^{\mathrm{NEP,hypo}} + F^{\mathrm{SED}}$), into their seasonal, trend, and residual components. The seasonal components were smoothed using a 7-d moving average filter to visualize seasonal patterns and differences between lakes. To let the seasonal components represent sources and sinks of DO, we added the long-term average to each seasonal component, which we estimated as the mean of the original time series minus the seasonal component of each flux, respectively. The range around each seasonal signal was calculated by decomposing the respective time series of the 97.5% and 2.5% quantiles. We further analyzed the temporal dynamics of the trend component time series of the total NEP flux including the 97.5% and 2.5% quantiles. To investigate differences between the lakes, we calculated the correlation coefficients between the total NEP trend time series and clustered the correlation coefficients using hierarchical clustering and the Ward method (Johnson and Wichern 2007).

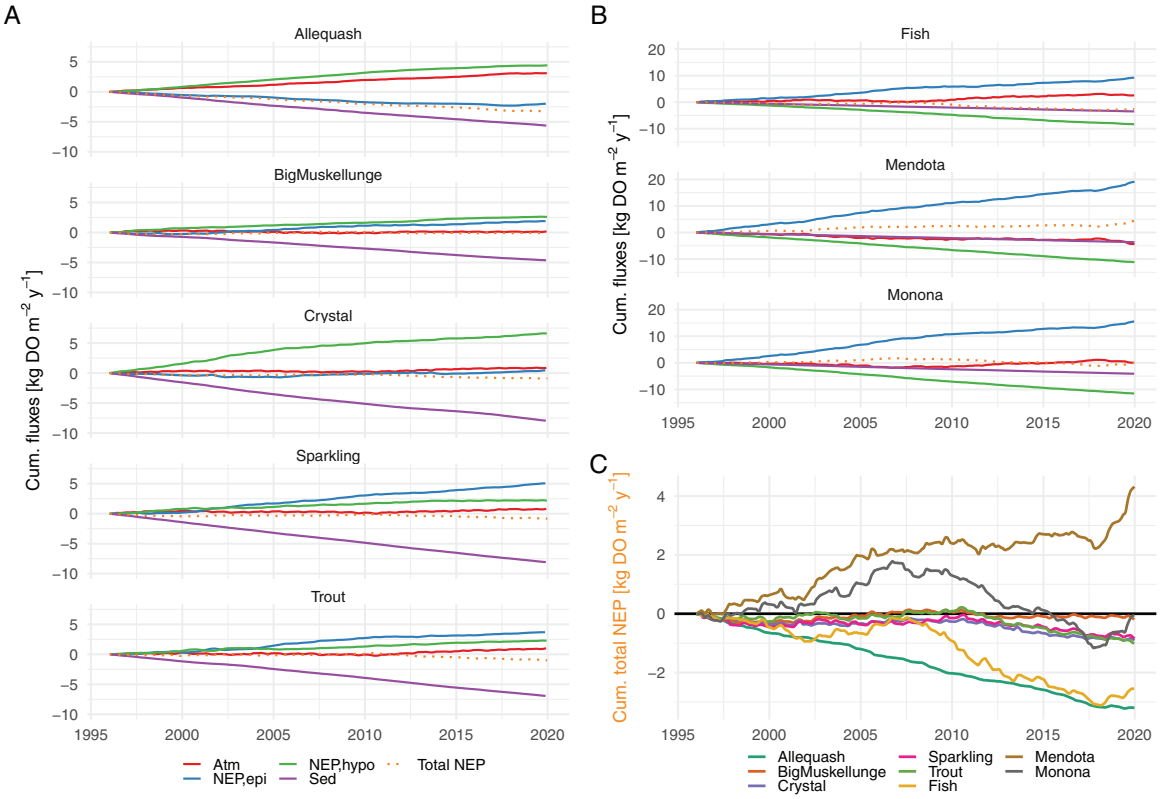

Fig. 4. Simulated, cumulative daily fluxes of atmospheric exchange (Atm), NEP in epilimnion (NEP,epi) and hypolimnion (NEP,hypo), sediment oxygen demand (Sed), and the total NEP flux, $F_{\text{total}}^{\text{NEP}}$, of the ecosystem as the sum of NEP and sediment oxygen demand fluxes of the eight NTL-LTER lakes over the time period when observed data were available for all study sites (starting in 1996 for the southern lakes). (**A**) Cumulative fluxes for the northern lakes. (**B**) Cumulative fluxes for the southern lakes. (**C**) Comparison of the cumulative total NEP fluxes for all study sites.

To quantify long-term changes in hypolimnetic DO depletion, we calculated the ratio between the simulated DO concentrations in the hypolimnion and the theoretical DO saturation concentration at the hypolimnion water temperature for each summer season (one per year) at each lake site. To provide an even temporal grid, the days of the year of each summer stratified period were given as a percentage of duration between 0 and 100 (hence, the start of summer stratification was 0 and the end of summer stratification was 100). This ensured that all seasonal time series were comparable for the purpose of clustering. Time series of ratios were smoothed using a 10-day moving average filter. Pooling all time series, we applied hierarchical clustering to identify the most common patterns using the Ward method. Three clusters were found to be the optimum number of clusters, as determined by the Elbow method, and the Average Silhouette method (Johnson and Wichern 2007).

Results

Model performance

As an example, the metabolism model's performance for Lake Mendota for 2003–2006 illustrates the agreement of simulated to observed DO data, and the ability of the model to capture annual summer depletion (Fig. 2, time series of simulated to observed DO for all lakes are in Supporting Information Figs. S4–S11). For Lake Mendota, the $X^{\text{NEP,epi}}$ and $X^{\text{NEP,hypo}}$ parameters had seasonal patterns (Fig. 2A). The hypolimnetic NEP parameter, $X^{\text{NEP,hypo}}$, along with the constant high sediment oxygen demand parameter, X^{SED}, contributed to summer DO consumption in the hypolimnion. NEP in the epilimnion increased during summer stratification (Fig. 2B). These fluxes determine the simulated DO concentrations (Fig. 2C) that show reoccurring seasonal patterns: (1) during summer stratification there are stable DO concentrations in the epilimnion (which can become variable due to primary production by phytoplankton), and a strong DO consumption signal in the hypolimnion; (2) replenishment of DO during the non-stratified period. The uncertainties around the parameters, fluxes and concentrations are higher during the mixed period as fewer data were available for the model parameter estimations.

Empirical X flux parameters were estimated when a lake mixing state shift occurred. These estimates, evident, for example, as an early negative summer peak of F_{SED} in 2003 (Fig. 2B), have an increased uncertainty as no field data were

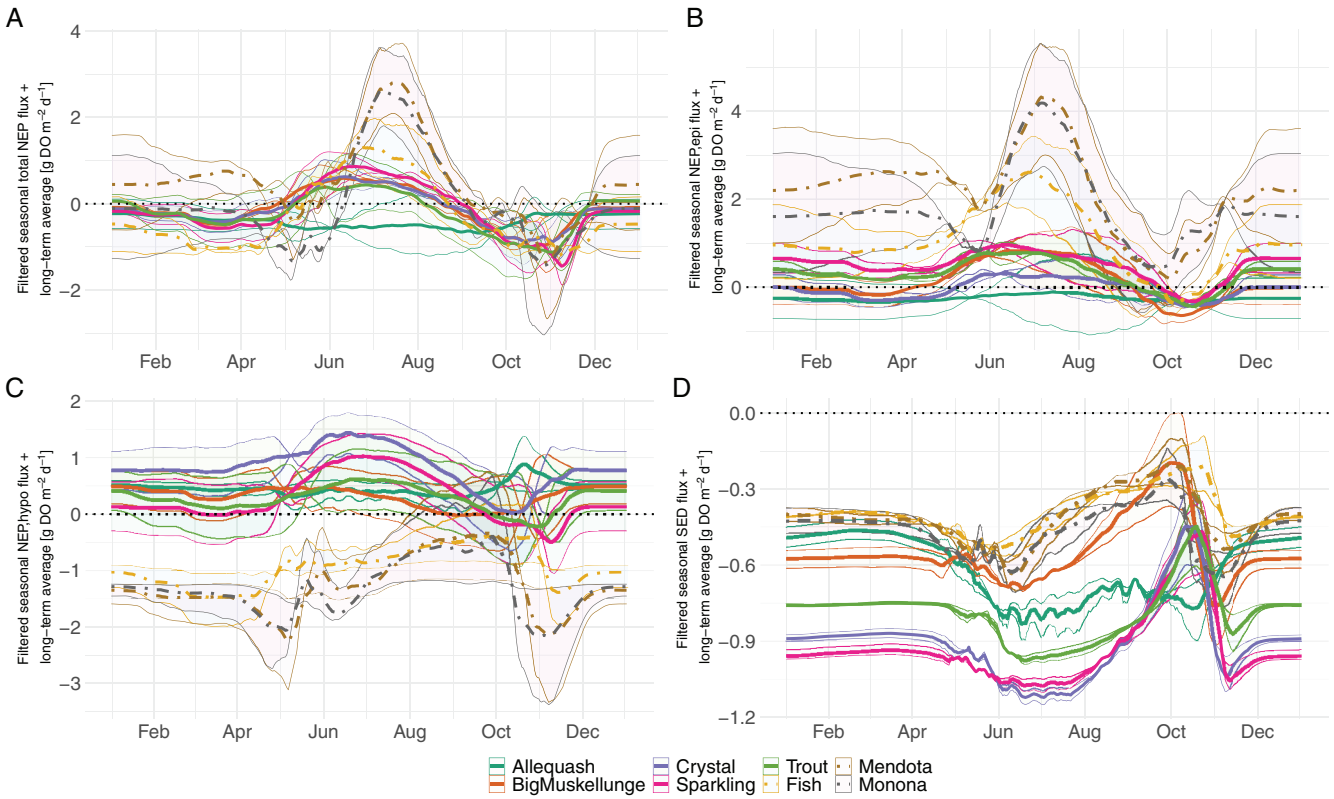

Fig. 5. Metabolism phenology represented by the seasonal signals of each lake. Each full time series (starting in 1981 for the northern lakes and in 1995/1996 for the southern lakes) was decomposed into the seasonal component to which the respective long-term average was added. solid lines represent filtered seasonal flux signals using a moving average filter with a window of 7 d for northern lakes, whereas dashed lines represent southern lakes. (**A**) Seasonal component of total NEP flux (F^{NEP}_{total}). (**B**) Seasonal component of NEP flux in epilimnion. (**C**) Seasonal component of NEP flux in hypolimnion. (**D**) Seasonal component of sediment oxygen demand flux.

available to verify the model's likelihood fit. Therefore, multiple simulated years have two apparent early peaks of hypolimnetic oxygen consumption—the first one when the flux parameters were estimated due to a lake mixing state shift with a high uncertainty around the flux values (Fig. 2B), and a second when the flux parameters were estimated from observational data. Modeled high DO consumption fluxes early in the stratified summer season are therefore model artifacts due to our choice of model parameter estimation.

Our metabolism model performed well on all lakes (Fig. 3). The southern lakes (Fig. 3, Fish, Mendota, and Monona) had a high proportion of measurements either at concentrations near 0 or ∼ 7–10 g DO m^{-3}, which highlighted the partitioning of the stratified layers of the southern eutrophic lakes. Seasonal anoxia or hypoxia in the hypolimnion resulted in concentrations around 0 g DO m^{-3}, and primary production as well as atmospheric exchange in the epilimnion are responsible for the high proportion of concentrations close to saturation. The metabolism model slightly overpredicted hypolimnetic DO in the southern, eutrophic Monona, hence the simulated hypolimnetic DO consumption is less than measured DO consumption. The model had lowest performance in replicating hypolimnetic DO in the shallow northern lake Allequash (Fig. 3).

Metabolism phenology

All northern lakes acted as long-term DO sinks (Fig. 4C). Generally, the long-term variability of the cumulative fluxes was higher for southern eutrophic lakes (Fig. 4B) than for the northern oligotrophic lakes (Fig. 4A). All northern lakes had cumulatively positive NEP fluxes in the hypolimnion (Fig. 4A). The magnitude of the sediment oxygen demand in the northern lakes was similar to the southern lakes, highlighting their similar net DO consumption during summer stratification. The southern lakes had high cumulative NEP fluxes in the epilimnion compared to the lakes in the north (Fig. 4B). The absolute cumulative fluxes of Big Muskellunge were the lowest across all lakes (Fig. 4C). Only Mendota had a constant long-term positive total NEP flux. Uncertainties for fluxes are shown in Supporting Information Figs. S12 and S13.

The seasonal signal of the total water column NEP flux ($F^{NEP}_{total} = F^{NEP,epi} + F^{NEP,hypo} + F^{SED}$, F_{SED} is always a negative term) highlights different magnitudes and timings between the northern and southern lakes (Fig. 5A). For clarity,

Supporting Information Figs. S14 and S15 plot the northern and southern lakes separately. The seasonal signal was isolated from the simulated time series by removing the trend and sub-seasonal variation. Furthermore, the long-term average was added to the seasonal component to illustrate if a lake acted as DO source or sink over a typical season. A positive total NEP flux, $F_{\text{total}}^{\text{NEP}}$, is an indicator for in-lake oversaturation of DO, whereas a negative $F_{\text{total}}^{\text{NEP}}$ indicates DO undersaturation.

During the first 3 months of a calendar year, which is the typical ice-covered period, all lakes except Mendota have negative total NEP fluxes (Fig. 5A). In early April, the total NEP fluxes of the northern lakes, except Allequash, increase and remain mostly positive until the end of August. The southern lakes, Mendota and Monona, have a minimum of the total NEP flux during spring mixing around May, while none of the northern lakes did. During summer stratification (June to August), the northern lakes had an earlier total NEP maximum than the southern lakes, although the later maxima of Mendota, Monona and Fish were more pronounced. All lakes were emitting DO to the atmosphere, except Allequash which had seasonal total fluxes below zero during summer. During fall mixing (October to November), all lakes had a negative total NEP flux, with the northern lakes having an earlier negative total NEP flux than the southern lakes. Fall DO consumption is the main negative total metabolism flux event for the northern lakes (Fig. 5A) other than Allequash, whereas the southern lakes experience two flux minima, one prior to stratification and one during fall mixing. All southern lakes had positive epilimnetic NEP fluxes throughout the year (Fig. 6B). In contrast, the northern lakes, except Allequash, mostly experience positive epilimnetic NEP fluxes during the summer months, with Sparkling and Trout being the exceptions, as both lakes had positive epilimnetic NEP fluxes during winter and spring. Crystal's epilimnetic NEP flux only becomes positive from May to September. The northern lakes have positive hypolimnetic NEP fluxes throughout the year (Fig. 5C), with the exception of Sparkling and Trout during fall turnover. Hypolimnetic NEP fluxes in the eutrophic (southern) lakes were set negative throughout the season with reduced hypolimnetic NEP fluxes during the stratified summer period. Sediment fluxes are similar for all southern lakes and decline over the course of summer stratification (as the consumption is coupled to the abundance of DO via a first-order kinetics approach) (Fig. 5D). Northern lakes had a higher variance regarding their sediment fluxes of DO, for example, Trout, Sparkling, and Crystal behave more uniformly, whereas Big Muskellunge reaches a peak of DO consumption earlier in the summer season.

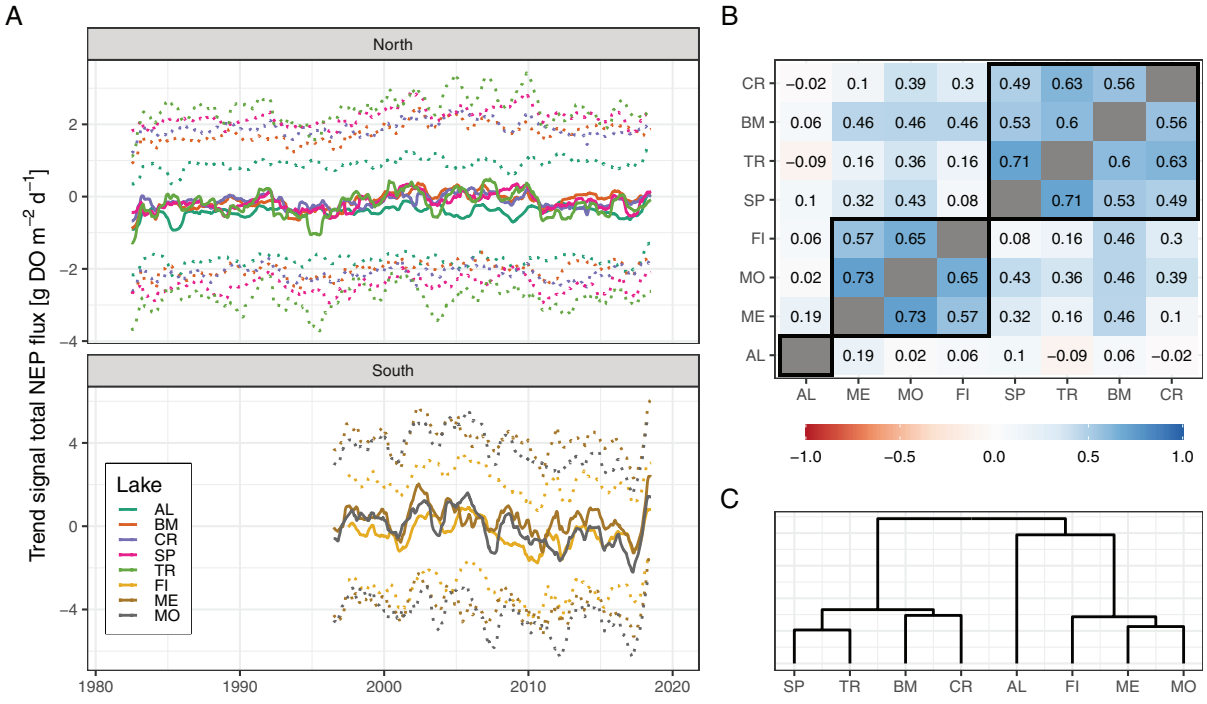

Fig. 6. Long-term changes and similarities in the total NEP flux, $F_{\text{total}}^{\text{NEP}}$, trends (AL, Allequash; BM, Big Muskellunge; CR, Crystal; SP, Sparkling; TR, Trout; ME, Mendota; MO, Monona; FI, Fish). (**A**) Scaled trends of the long-term total NEP fluxes for the northern (top) and southern (bottom) lakes. Dotted lines represent maximum and minimum scaled trend signals of the long-term total NEP fluxes, respectively (97.5% and 2.5% quantiles). (**B**) Correlation matrix of the trend component of the decomposed total NEP fluxes highlighting similarities between the study sites from red (negative correlation) to blue (positive correlation). Black squares represent clusters of positive correlations between the sites, which were identified using hierarchical clustering. (**C**) Dendrogram of the clusters that were identified using hierarchical clustering.

Long-term metabolic changes

The trend components of the total NEP flux time series fall into two distinct groupings, representing either the northern or southern regions (Fig. 6). The northern trends exhibit an elevated signal in their total NEP flux trend signal from 2000 until 2010 compared to other periods, as well as slightly overall reduced values since 2010 (Fig. 6A). Allequash is an exception and had low or negative correlated patterns to the trend dynamics of most northern lakes. The total NEP trend dynamics of the southern lakes behave more uniformly with a visible long-term decline over the period 2001–2018 indicating increased consumption of DO over time. The correlation matrix shows that the southern lakes have similar long-term trends (Fig. 6B). The northern lakes, except Allequash, also had similar correlation patterns, with Sparkling and Trout having the strongest correlation to each other among all northern lakes (Fig. 6B,C). Northern lakes had positive correlations of their long-term total NEP trends to the soulakes, except for Allequash.

Regional hypolimnetic oxygen phenology

Clustered ratios of hypolimnetic DO to saturation concentration had three distinct patterns of DO consumption during summer stratification (Fig. 7A):

Concave pattern: Low DO consumption through the first 50% of the summer, with DO concentrations slightly above saturation; DO consumption increases at the end of summer stratification and reaching near hypoxic conditions. This cluster was mainly observed in Crystal (Fig. 7B) and once in Sparkling and Trout, respectively.

Linear pattern: Linear DO depletion after stratification onset, stronger at the end of summer reaching low DO conditions.

Convex pattern: Exponential DO decrease after stratification onset; DO is fully consumed by about 50% of the summer period.

The northern lakes mostly had linear DO consumption patterns during summer stratification (Fig. 7B), characterized by a slow but steady depletion of DO over the course of summer. Allequash and Big Muskellunge had individual years with seasonal convex patterns. Crystal shifted from the concave pattern (1980s to early 2000s) recently to the linear consumption pattern. The southern lakes are all characterized by convex hypolimnetic DO consumption patterns throughout the observed period.

Discussion

Long-term metabolism estimates afford the opportunity to characterize seasonal patterns and evaluate them within the conceptual framework of phenology. Metabolism phenology is related to characteristics, such as trophic status, plankton community succession, lake mixing, and seasonal temperature patterns, as well as landscape and climatic setting. Long-term change in metabolism phenology is complicated, and some of the metabolic changes in our study lakes appear to be owed to impaired water quality. Although long-term change may not be attributable to a single cause, and the potential drivers of change differ among lakes, there are clues in the long-term patterns of correlates representing land use and climate. Metabolism phenology appears to be diverse for the lakes in northern

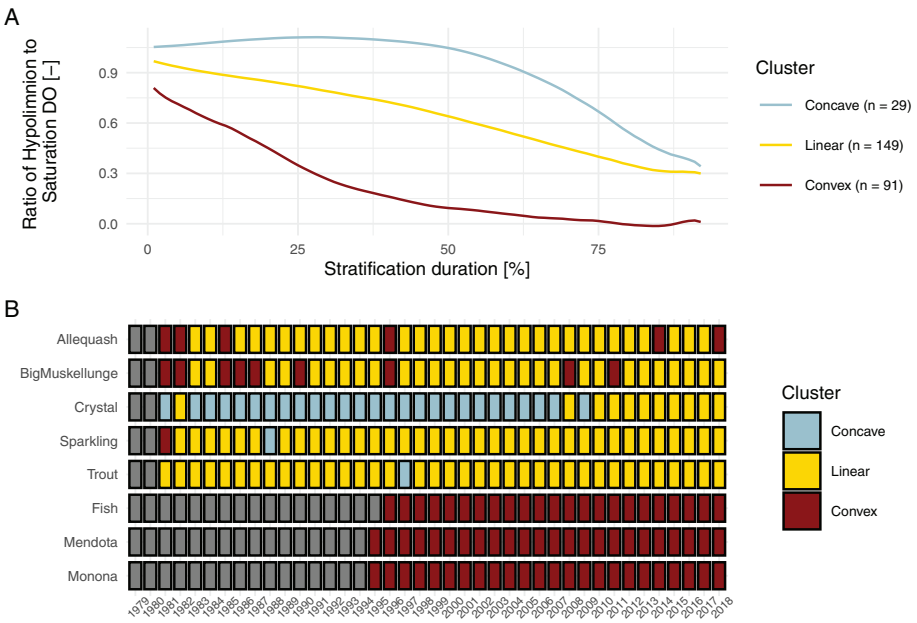

Fig. 7. Clustered idealized patterns of DO consumption in the hypolimnion over the course of a summer stratification period. (**A**) Smoothed ratios of hypolimnion to saturation DO concentrations over the summer stratification period. Each line represents one specific cluster. (**B**) Classification of each lake's seasonal hypolimnetic DO consumption according to the five established clusters (gray color represents years without field data).

Wisconsin, as control over DO is expressed by the balances of physical, chemical, and biological processes among the lakes. Lakes in southern Wisconsin share a more consistent metabolism phenology that is related to seasonal phytoplankton succession and persistent year-to-year hypolimnetic anoxia. These regional differences set the stage for interpretation of lake metabolism phenology as an emergent property that integrates ecological function in lakes and that provides insights into the potential effects of nutrient inputs from the landscape and changing climate on lake metabolism.

Metabolism phenology

The metabolism patterns of the eutrophic lakes in the south, Mendota and Monona, were associated with established patterns of phytoplankton and zooplankton seasonal succession during the open water season. Although an empirical analysis of plankton community succession is beyond the scope of this study, metabolism patterns in the eutrophic lakes map onto the conceptual model of the Phytoplankton Ecology Group (PEG; Sommer et al. 1986). We use Mendota as an example, following the analysis of phytoplankton succession by Carey et al. (2016) (Fig. 5; Supporting Information Fig. S15). Late winter and early spring blooms of *Chlorophyta* and *Bacilliariophyta*, along with low water clarity, indicate primary production in excess of respiration (similar to high total NEP fluxes during summer, *see* Fig. 5A). With warming temperatures and ample food, *Daphnia* biomass peaks in May, and graze phytoplankton to low abundance, increasing water clarity and raising respiration in excess of primary production, that is, slightly negative total NEP in April/May (Fig. 5A). This clear-water phase typically lasts until mid to late June (Matsuzaki et al. 2021), when periodic cyanobacterial blooms foreshadow a switch to the algal dominated phase, which persists through early autumn, when total NEP is positive in the eutrophic lakes. Fall mixing increases nutrients in the water column, which help maintain high phytoplankton abundance through the remainder of the open water season. The PEG model generally predicts two or more phytoplankton peaks—diatoms in spring and fall, and Cyanobacteria in summer—and lakes Mendota and Monona had this trimodal pattern of high epilimnetic NEP (Fig. 5B). Factors other than phytoplankton succession appear important, as well, and these are discussed in the comparison of sediment and water column metabolism.

Sediment metabolism provides additional insights into the metabolism phenology of southern lakes. Persistent summer algal blooms (Lathrop 2007) explain the consistent epilimnetic NEP patterns as well as hypolimnetic NEP and sediment oxygen demand. Export of epilimnetic phytoplankton biomass to the hypolimnion and sediments increases organic matter accumulation (McCullough et al. 2018), provides excess substrate that fuels microbial respiration (Hoffman et al. 2013), and leads to recurrent anoxia (Sobek et al. 2009). Although Fish Lake has a mesotrophic TP concentration (Table 1), its sediment oxygen demand (Fig. 5D) and hypolimnetic oxygen depletion (Fig. 7B) indicate eutrophy. Due to Fish's location in a watershed which is dominated by agricultural land use, and that the lake is a closed basin, sediment oxygen demand may be fueled by high allochthonous organic matters loads.

Oligotrophic lakes have a more diverse set of seasonal metabolism patterns (Fig. 5; Supporting Information Fig. S14). Lake metabolism does not map directly onto the PEG model of phytoplankton and zooplankton community succession. While chlorophyll *a* concentrations generally peak in the spring in most oligotrophic lakes in this study (data not shown, but available at Magnuson et al. 2020*b*), total NEP tends to be stable through spring and then peaks during summer (Fig. 5A). The cumulative DO fluxes (Fig. 4A), the seasonal metabolism patterns (Fig. 5A), and the hypolimnetic DO consumption patterns (Fig. 7B) all show slight differences among the lakes, despite similarities in nutrient concentrations (Table 1). Hydrology may explain some of the differences, as the two lakes with substantial surface water inputs and the shortest hydrologic RTs, Allequash, and Trout, are the northern lakes with the lowest total NEP fluxes. Allequash's low hydrologic RT suggests its organic carbon budget may be dominated by allochthonous sources (Hotchkiss et al. 2018), which would, in turn, lower NEP. In addition, Allequash has the lowest overall seasonal dynamics of NEP in the epilimnion and hypolimnion, which fits other work showing low inter-annual variability in metabolism in drainage lakes (Oleksy et al. 2021). In addition to other factors (e.g., high organic carbon loads, irregular shape, drainage lake), potential polymixis in Allequash during its weakly stratified summer period may lead to a model bias regarding seasonal DO dynamics. Occasional mixing events would violate the assumptions of our two-layer metabolism model for the summer period as our model assumes the water column to be stratified. The inference for oligotrophic lakes is that metabolism phenology may be more influenced by the physical–chemical–biological interactions that define each lake's ecology. Lake metabolism phenology may be one more example of how lake diversity is suppressed by eutrophication (Hautier et al. 2009; Qin et al. 2013; Glibert 2017) as the metabolism phenology of southern, eutrophic lakes behaves more uniformly.

Within-lake spatial heterogeneity may account for some differences observed in metabolism phenology, especially in the northern lakes. Our model does not explicitly account for littoral-benthic metabolic processes and likely biases the planktonic-offshore DO measurements (Brothers and Vadeboncoeur 2021). Any contributions of littoral planktonic, periphyton and submerged macrophyte activity to pelagic DO dynamics, via lateral flow processes, are subsumed in our general metabolism analysis and evaluation. Depending on the degree of mixing, littoral signals may largely be missed (Lauster et al. 2006; Van de Bogert et al. 2007; Cavalcanti et al. 2016). This bias to pelagic metabolism could oversimplify in-

lake metabolism phenology. Future work that either filters diel DO measurements to compensate for vertical motions (Castro et al. 2021), or that incorporates littoral measurements and lateral DO transport would provide new and potentially valuable insights to lake metabolism phenology.

Temporal coherence and long-term changes of lake metabolism

Landscape setting shapes regional differences in long-term changes in metabolism fluxes. The relatively moderate temporal coherence across all lakes (north and south) suggests a limited influence of climate on lake metabolism and suggests that temporal coherence of long-term metabolism change is driven primarily by local factors (Fig. 6). Magnuson et al. (1990) stated that coherence of lake variables among the NTL-LTER lakes does not appear to be related to area, depth, or hydrologic RT, as might be expected, but rather to trophic state, which is an outcome principally of historical land use practices for these lakes (Carpenter et al. 2007). Temporal coherence of in-lake processes to local catchment variables found in previous work (Feuchtmayr et al. 2012; Lodi et al. 2018; Walter et al. 2020) is consistent with our findings of high within-region correlation of the trend of total NEP fluxes (Fig. 6B). Although lakes in their respective regions behaved more uniformly, the trend components of total NEP fluxes were positively correlated across all investigated lakes (except Allequash). This indicates a possible climate component to temporal coherence (Benson et al. 2000; Palmer et al. 2014; Magee and Wu 2017*b*). Although climate may be secondary in its influence of coherence, future studies that focus on different time scales of change or on interactions of climate and land use may reveal new patterns of influence by climate on long-term lake metabolism. Future work that investigates the entanglement of long-term atmospheric nutrient deposition rates with in-lake metabolism change is intriguing, as increasing nitrogen and/or phosphorus deposition rates could explain potential metabolism changes (Jassby et al. 1994; Anderson and Downing 2006; Bergström and Jansson 2006).

Hypolimnetic metabolism has important ecological implications. Southern lakes have had the same pattern of hypolimnetic DO consumption for the past 20 years (Fig. 7B). There is little inter-annual variation, probably because high accumulation rates of organic matter in sediments elevate ecosystem respiration well beyond primary production (McCullough et al. 2018), and respiration is likely not substrate limited (Hoffman et al. 2013). Inter-annual variation in the relative magnitude of hypolimnetic DO consumption (e.g., Mendota) is better explained by physical factors, such as the strength of thermal stratification (Ladwig et al. 2021). In the north, hypolimnetic DO consumption gave rise to three distinct seasonal patterns (Fig. 7A). The concave pattern indicates positive NEP in the hypolimnion for the first 1–2 months of stratification (e.g., Crystal), and likely indicates substantial primary production below the thermocline. Allequash and Big Muskellunge occasionally switched in their hypolimnetic DO patterns from linear to convex (Fig. 7B), whereas Crystal shifted from concave to linear patterns. In 2012–2013, Crystal underwent a whole lake mixing experiment, in which hypolimnetic water temperatures were artificially warmed and oxygenated (Lawson et al. 2015), though the reported changes preceded this experiment. Changes in water clarity (Rose et al. 2016) may explain some of the changes in Crystal, where water clarity has declined since the 1980s, which results in warming surface waters but colder bottom waters. In contrast, clarity in Sparkling has not been changing since the 1980s resulting in concurrent warming of surface and bottom waters. Such site-specific water clarity trends can affect mixing and eventually DO dynamics (Jane et al. 2021).

Metabolism modeling framework

All numerical models strike a balance between process over-simplification and over-parameterization. The pronounced vertical thermal gradient in our study lakes allowed focus on vertical exchange of DO between atmosphere, epilimnion and hypolimnion and to neglect lateral fluxes. Our metabolism model, with a simplified two-layer structure, performed well in replicating both long-term and seasonal dynamics of the observed DO, in part because the Bayesian framework incorporated the observational data. Though we used daily output from a hydrodynamic lake model to calculate daily DO values, the resolution of our results is coarser than in most metabolism studies that use high-frequency DO measurements (Staehr et al. 2012*a*). It would be reasonable to assume our model would capture fewer extreme metabolism-related events, such as short-term phytoplankton blooms (Batt et al. 2017; Carpenter et al. 2020). We envision that our metabolism model may be adapted for other dimictic lake systems that have a long-term record of water temperature and DO measurements.

Our model results for hypolimnetic DO fluxes form a basis of comparison to other approaches (see Supporting Information "Comparison of estimated hypolimnetic metabolic fluxes with alternative approaches"). Although fundamental differences in methodology confound direct quantitative comparison, we provide a qualitative comparison. Furthermore, we recognize that the uncertainty in our estimates depends on the equations of the process-based model and observed DO data, and that uncertainty can be high for correlated parameters. This dilemma, known as equifinality, is a general challenge for the optimization of mathematical models (Beven 2006). Our approach to restrict hypolimnetic NEP parameter values to a negative range for eutrophic lakes contributed to the reasonably good agreement between DO consumption estimates by the deductive model of Livingstone and Imboden (1996) and our modeled metabolism fluxes (Supporting Information Fig. S3; see Supporting Information "Comparison of

estimated hypolimnetic metabolic fluxes with alternative approaches") of the southern lakes. For northern lakes, our modeled estimates for hypolimnetic NEP were similar to the primary productivity estimates from ^{14}C data when including primary productivity in the metalimnion.

Conclusions

Observations of DO in lakes remain as relevant today for providing insights to ecological function as they had been more than a century ago (Birge 1910). Through sequential modeling, we use observational data and a hydrodynamic model to create dynamical lake states for two thermal layers, and from those states we model metabolism in thermal strata to quantify DO fluxes within the lake. From these flux patterns, we decompose seasonal metabolism phenology and use time-series analysis to explore its long-term change. This sequence of abstractions provides for mathematically reproducible connections between field observations and long-term ecosystem function, from which inferences of long-term change can be explored. The metabolism results in this study agreed with field data and additional known ecosystem patterns, such as seasonal phytoplankton succession. Time-series analysis highlighted landscape-related differences between the forested lakes in the north and the agricultural/urban lakes in the south, which are likely related to trophic states as well as flow regimes. All lakes had a stronger long-term temporal coherence of total net ecosystem productivity related to their landscape setting than to climate. For the southern eutrophic lakes, long-term DO consumption is increasing, and water management should adapt accordingly for future water quality deterioration. Our study highlights long-term metabolism changes but stops short of evaluating or identifying causal drivers behind long-term metabolism patterns. Future work should focus on establishing causal relationships between long-term data, climate variables, water quality, hydrologic fluxes, and catchment characteristics, relative to metabolism fluxes to improve understanding of metabolism phenology across different lake types. A better understanding of causation can advance understanding of ecosystem function, and will accelerate the application of lake metabolism to water management strategies (Jankowski et al. 2021).

Data availability statement

Script, model configurations, and outputs to process the data are archived and available at the Environmental Data Initiative portal (Ladwig et al. 2022, https://doi.org/10.6073/pasta/af991c26bace5af8d4b3bb66d7b18af7) as well as on Zenodo (https://doi.org/10.5281/zenodo.6363561). All NTL-LTER data are cited in the references and are available via the Environmental Data Initiative (https://environmentaldatainitiative.org).

References

Anderson, K. A., and J. A. Downing. 2006. Dry and wet atmospheric deposition of nitrogen, phosphorus and silicon in an agricultural region. Water Air Soil Pollut. **176**: 351–374. doi:10.1007/s11270-006-9172-4

Appling, A. P., R. O. Hall, C. B. Yackulic, and M. Arroita. 2018. Overcoming equifinality: Leveraging long time series for stream metabolism estimation. J. Geophys. Res. Biogeosci. **123**: 624–645. doi:10.1002/2017JG004140

Batt, R. D., S. R. Carpenter, and A. R. Ives. 2017. Extreme events in lake ecosystem time series. Limnol. Oceanogr. Lett. **2**: 63–69. doi:10.1002/lol2.10037

Benson, B. J., J. D. Lenters, J. J. Magnuson, M. Stubbs, T. K. Kratz, P. J. Dillon, R. E. Hecky, and R. C. Lathrop. 2000. Regional coherence of climatic and lake thermal variables of four lake districts in the Upper Great Lakes region of North America: Regional coherence of climatic and lake thermal variables. Freshw. Biol. **43**: 517–527. doi:10.1046/j.1365-2427.2000.00572.x

Bergström, A.-K., and M. Jansson. 2006. Atmospheric nitrogen deposition has caused nitrogen enrichment and eutrophication of lakes in the northern hemisphere. Glob. Chang. Biol. **12**: 635–643. doi:10.1111/j.1365-2486.2006.01129.x

Beven, K. 2006. A manifesto for the equifinality thesis. J. Hydrol. **320**: 18–36. doi:10.1016/j.jhydrol.2005.07.007

Birge, E. A. 1910. Gases dissolved in the waters of Wisconsin lakes. Bull. Bur. Fish. **28**: 1273–1294.

Bouffard, D., and A. Wüest. 2019. Convection in lakes. Annu. Rev. Fluid Mech. **51**: 189–215. doi:10.1146/annurev-fluid-010518-040506

Brothers, S., and Y. Vadeboncoeur. 2021. Shoring up the foundations of production to respiration ratios in lakes. Limnol. Oceanogr. **9999**: 1–17. doi:10.1002/lno.11787

Burchard, H., K. Bolding, and M. R. Villarreal. 1999. GOTM, a general ocean turbulence model: Theory, implementation and test cases. European Commission, Join Research Centre, Space Applications Institute, Space Applications Institute.

Butterworth, B. J., and S. D. Miller. 2016. Air–sea exchange of carbon dioxide in the Southern Ocean and Antarctic marginal ice zone. Geophys. Res. Lett. **43**: 7223–7230. doi:10.1002/2016GL069581

Carey, C. C., P. C. Hanson, R. C. Lathrop, A. L. St, and Amand. 2016. Using wavelet analyses to examine variability in phytoplankton seasonal succession and annual periodicity. J. Plankton Res. **38**: 27–40. doi:10.1093/plankt/fbv116

Carey, C. C., J. P. Doubek, R. P. McClure, and P. C. Hanson. 2018. Oxygen dynamics control the burial of organic carbon in a eutrophic reservoir: Oxygen dynamics control OC burial. Limnol. Oceanogr. Lett. **3**: 293–301. doi:10.1002/lol2.10057

Carpenter, S. R., and others. 2007. Understanding regional change: A comparison of two lake districts. Bioscience **57**: 323–335. doi:10.1641/B570407

Carpenter, S. R., B. M. S. Arani, P. C. Hanson, M. Scheffer, E. H. Stanley, and E. Van Nes. 2020. Stochastic dynamics of cyanobacteria in long-term high-frequency observations of a eutrophic lake. Limnol. Oceanogr. Lett. **5**: lol2.10152. doi:10.1002/lol2.10152

Castro, B.,. F., H. E. Chmiel, C. Minaudo, S. Krishna, P. Perolo, S. Rasconi, and A. Wüest. 2021. Primary and net ecosystem production in a large lake diagnosed from high-resolution oxygen measurements. Water Resour. Res. **57**: 1–24. doi:10.1029/2020WR029283

Cavalcanti, J. R., D. da Motta-Marques, and C. R. Fragoso Jr. 2016. Process-based modeling of shallow lake metabolism: Spatio-temporal variability and relative importance of individual processes. Ecol. Model. **323**: 28–40. doi:10.1016/j.ecolmodel.2015.11.010

Cole, J. J., M. L. Pace, S. R. Carpenter, and J. F. Kitchell. 2000. Persistence of net heterotrophy in lakes during nutrient addition and food web manipulations. Limnol. Oceanogr. **45**: 1718–1730. doi:10.4319/lo.2000.45.8.1718

Coloso, J. J., J. J. Cole, P. C. Hanson, and M. L. Pace. 2008. Depth-integrated, continuous estimates of metabolism in a clear-water lake. Can. J. Fish. Aquat. Sci. **65**: 712–722. doi:10.1139/f08-006

Dugan, H. A., and others. 2016. Consequences of gas flux model choice on the interpretation of metabolic balance across 15 lakes. Inland Waters **6**: 581–592. doi:10.1080/IW-6.4.836

Feuchtmayr, H., S. J. Thackeray, I. D. Jones, M. De Ville, J. Fletcher, B. James, and J. Kelly. 2012. Spring phytoplankton phenology—Are patterns and drivers of change consistent among lakes in the same climatological region? Drivers of phytoplankton phenology in four lakes. Freshw. Biol. **57**: 331–344. doi:10.1111/j.1365-2427.2011.02671.x

Garcia, H., and L. Gordon. 1992. Oxygen solubility in seawater: Better fitting equations. Limnol. Oceanogr. **37**: 1307–1312.

Giling, D. P., and others. 2017. Delving deeper: Metabolic processes in the metalimnion of stratified lakes. Limnol. Oceanogr. **62**: 1288–1306. doi:10.1002/lno.10504

Glibert, P. M. 2017. Eutrophication, harmful algae and biodiversity—Challenging paradigms in a world of complex nutrient changes. Mar. Pollut. Bull. **124**: 591–606. doi:10.1016/j.marpolbul.2017.04.027

Goudsmit, G.-H., H. Burchard, F. Peeters, and A. Wüest. 2002. Application of k-ϵ turbulence models to enclosed basins: The role of internal seiches. J. Geophys. Res. Oceans **107**: 3230. doi:10.1029/2001JC000954

Hamilton, D. P., and S. G. Schladow. 1997. Prediction of water quality in lakes and reservoirs. Part I—Model description. Ecol. Model. **96. 1**: 91–110. doi:10.1016/S0304-3800(96)00062-2

Han, P., and D. M. Bartels. 1996. Temperature dependence of oxygen diffusion in H_2O and D_2O. J. Phys. Chem. **100**: 5597–5602. doi:10.1021/jp952903y

Hanson, P. C., D. L. Bade, S. R. Carpenter, and T. K. Kratz. 2003. Lake metabolism: Relationships with dissolved organic carbon and phosphorus. Limnol. Oceanogr. **48**: 1112–1119. doi:10.4319/lo.2003.48.3.1112

Hanson, P. C., D. P. Hamilton, E. H. Stanley, N. Preston, O. C. Langman, and E. L. Kara. 2011. Fate of allochthonous dissolved organic carbon in lakes: A quantitative approach. PLoS One **6**: e21884. doi:10.1371/journal.pone.0021884

Hautier, Y., P. A. Niklaus, and A. Hector. 2009. Competition for light causes plant biodiversity loss after eutrophication. Science **324**: 636–638. doi:10.1126/science.1169640

Heiskanen, J. J., I. Mammarella, S. Haapanala, J. Pumpanen, R. Vesala, S. MacIntyre, and A. Ojala. 2014. Effects of cooling and internal wave motions on gas transfer coefficients in a boreal lake. Tellus B **66**: 22826. doi:10.3402/tellusb.v66.22827

Hipsey, M. R., and others. 2019. A general lake model (GLM 3.0) for linking with high-frequency sensor data from the Global Lake Ecological Observatory Network (GLEON). Geosci. Model Dev. **12**: 473–523. doi:10.5194/gmd-12-473-2019

Hoellein, T. J., D. A. Bruesewitz, and D. C. Richardson. 2013. Revisiting Odum (1956): A synthesis of aquatic ecosystem metabolism. Limnol. Oceanogr. **58**: 2089–2100. doi:10.4319/lo.2013.58.6.2089

Hoffman, A. R., D. E. Armstrong, and R. C. Lathrop. 2013. Influence of phosphorus scavenging by iron in contrasting dimictic lakes. Can. J. Fish. Aquat. Sci. **70**: 941–952. doi:10.1139/cjfas-2012-0391

Holtgrieve, G. W., D. E. Schindler, T. A. Branch, and Z. T. A'mar. 2010. Simultaneous quantification of aquatic ecosystem metabolism and reaeration using a Bayesian statistical model of oxygen dynamics. Limnol. Oceanogr. **55**: 1047–1063. doi:10.4319/lo.2010.55.3.1047

Hondzo, M., and H. G. Stefan. 1993. Lake water temperature simulation model. J. Hydraul. Eng. **119**: 1251–1273. doi:10.1061/(ASCE)0733-9429(1993)119:11(1251)

Hotchkiss, E. R., S. Sadro, and P. C. Hanson. 2018. Toward a more integrative perspective on carbon metabolism across lentic and lotic inland waters. Limnol. Oceanogr. Lett. **3**: 57–63. doi:10.1002/lol2.10081

Imberger, J., and P. F. Hamblin. 1982. Dynamcis of lakes, reservoirs, and cooling ponds. Annu. Rev. Fluid Dyn. **14**: 153–187. doi:10.1146/annurev.fl.14.010182.001101

Jansen, J., and others. 2021. Winter limnology: How do hydrodynamics and biogeochemistry shape ecosystems under ice? J. Geophys. Res. Biogeosci. **126**: 6. doi:10.1029/2020JG006237

Janssen, A. B. G., and others. 2015. Exploring, exploiting and evolving diversity of aquatic ecosystem models: A community perspective. Aquat. Ecol. **49**: 513–548. doi:10.1007/s10452-015-9544-1

Janssen, A. B. G., and others. 2019. PCLake+: A process-based ecological model to assess the trophic state of stratified and

non-stratified freshwater lakes worldwide. Ecol. Model. **396**: 23–32. doi:10.1016/j.ecolmodel.2019.01.006

Jane, S. F., and others. 2021. Widespread deoxygenation of temperate lakes. Nature **594**: 66–70. doi:10.1038/s41586-021-03550-y

Jankowski, K. J., F. H. Mejia, J. R. Blaszczak, and G. W. Holtgrieve. 2021. Aquatic ecosystem metabolism as a tool in environmental management. WIREs Water **8**: 1–27. doi:10.1002/wat2.1521

Jassby, A. D., J. E. Reuter, R. P. Axler, C. R. Goldman, and S. H. Hackley. 1994. Atmospheric deposition of nitrogen and phosphorus in the annual nutrient load of Lake Tahoe (California-Nevada). Water Resour. Res. **30**: 2207–2216. doi:10.1029/94WR00754

Jenny, J.-P., and others. 2016. Urban point sources of nutrients were the leading cause for the historical spread of hypoxia across European lakes. Proc. Natl. Acad. Sci. **113**: 12655–12660. doi:10.1073/pnas.1605480113

Johnson, R. A., and D. W. Wichern. 2007. Applied multivariate statistical analysis, 6th ed. Pearson Education, Inc.

Jørgensen, B. B., and N. P. Revsbech. 1985. Diffusive boundary layers and the oxygen uptake of sediments and detritus1: Diffusive boundary layers. Limnol. Oceanogr. **30**: 111–122. doi:10.4319/lo.1985.30.1.0111

Kamarainen, A. M., R. M. Penczykowski, M. C. Van de Bogert, P. C. Hanson, and S. R. Carpenter. 2009. Phosphorus sources and demand during summer in a eutrophic lake. Aquat. Sci. **71**: 214–227. doi:10.1007/s00027-009-9165-7

Ladwig, R., P. C. Hanson, H. A. Dugan, C. C. Carey, Y. Zhang, L. Shu, C. J. Duffy, and K. M. Cobourn. 2021. Lake thermal structure drives inter-annual variability in summer anoxia dynamics in a eutrophic lake over 37 years. Hydrol. Earth Syst. Sci. **25**: 1009–1032. doi:10.5194/hess-2020-349

Ladwig, R., A. P. Appling, A. Delany, H. A. Dugan, Q. Gao, N. Lottig, J. Stachelek, and P. C. Hanson. 2022. Modeling dataset: Long-term change in metabolism phenology across north-temperate lakes, Wisconsin, USA 1979-2019 ver 1. Environmental Data Initiative. doi:10.6073/pasta/af991c26bace5af8d4b3bb66d7b18af7

Lathrop, R. C. 2007. Perspectives on the eutrophication of the Yahara lakes. Lake Reserv.Manage. **23**: 345–365. doi:10.1080/07438140709354023

Lathrop, R., and S. Carpenter. 2014. Water quality implications from three decades of phosphorus loads and trophic dynamics in the Yahara chain of lakes. Inland Waters **4**: 1–14. doi:10.5268/IW-4.1.680

Lauster, G. H., P. C. Hanson, and T. K. Kratz. 2006. Gross primary production and respiration differences among littoral and pelagic habitats in northern Wisconsin lakes. Can. J. Fish. Aquat. Sci. **63**: 1130–1141. doi:10.1139/F06-018

Lawson, Z. J., M. J. Vander Zanden, C. A. Smith, E. Heald, T. R. Hrabik, and S. R. Carpenter. 2015. Experimental mixing of a north-temperate lake: Testing the thermal limits of a cold-water invasive fish. Can. J. Fish. Aquat. Sci. **72**: 926–937. doi:10.1139/cjfas-2014-0346

Liu, H., H. Wang, N. Li, J. Shao, X. Zhou, K. J. van Groenigen, and M. P. Thakur. 2022. Phenological mismatches between above- and belowground plant responses to climate warming. Nat. Clim. Change **12**: 97–102. doi:10.1038/s41558-021-01244-x

Livingstone, D. M., and D. M. Imboden. 1996. The prediction of hypolimnetic oxygen profiles: A plea for a deductive approach. Can. J. Fish. Aquat. Sci. **53**: 924–932. doi:10.1139/f95-230

Lodi, S., L. F. Machado-Velho, P. Carvalho, and L. M. Bini. 2018. Effects of connectivity and watercourse distance on temporal coherence patterns in a tropical reservoir. Environ. Monit. Assess. **190**: 566. doi:10.1007/s10661-018-6902-1

Lovely, A., and others. 2015. The gas transfer through Polar Sea ice experiment: Insights into the rates and pathways that determine geochemical fluxes. Geophys. Res. Oceans **120**: 8177–8194. doi:10.1002/2014JC010607

Luo, L., D. Hamilton, J. Lan, C. McBride, and D. Trolle. 2018. Autocalibration of a one-dimensional hydrodynamic-ecological model (DYRESM 4.0-CAEDYM 3.1) using a Monte Carlo approach: Simulations of hypoxic events in a polymictic lake. Geosci. Model Dev. **11**: 903–913. doi:10.5194/gmd-11-903-2018

MacIntyre, S., and J. M. Melack. 1995. Vertical and horizontal transport in lakes: Linking littoral, benthic and pelagic habitats. J North Am. Benthol. Soc. **14**: 599–615. doi:10.2307/1467544

MacIntyre, S., A. Jonsson, M. Jansson, J. Aberg, D. E. Turney, and S. D. Miller. 2010. Buoyancy flux, turbulence, and the gas transfer coefficient in a stratified lake. Geophys. Res. Lett. **37**: L24604.

MacIntyre, S., J. H. Amaral, and J. M. Melack. 2021. Turbulence in the upper mixed layer under light winds: Implications for fluxes of climate-warming trace gases. J. Geophys. Res. Oceans **126**: e2020JC017026.

Magee, M. R., and C. H. Wu. 2017*a*. Effects of changing climate on ice cover in three morphometrically different lakes: Climate change on ice cover in three morphometrically different lakes. Hydrol. Process. **31**: 308–323. doi:10.1002/hyp.10996

Magee, M. R., and C. H. Wu. 2017*b*. Response of water temperatures and stratification to changing climate in three lakes with different morphometry. Hydrol. Earth Syst. Sci. **21**: 6253–6274. doi:10.5194/hess-21-6253-2017

Magnuson, J. J., B. J. Benson, and T. K. Kratz. 1990. Temporal coherence in the limnology of a suite of lakes in Wisconsin, U.S.A. Freshw. Biol. **23**: 145–159. doi:10.1111/j.1365-2427.1990.tb00259.x

Magnuson, J. J., T. K. Kratz, and B. J. Benson. 2006. Long-term dynamics of lakes in the landscape: Long-term ecological research on north temperate lakes. Oxford Univ. Press.

Magnuson, J. J., S. R. Carpenter, and E. H. Stanley. 2013. North temperate lakes LTER northern highland lake district Bathymetry ver 2. Environmental Data Initiative. doi: 10.6073/pasta/fb60afe5bbed735f8ca2316c1ca38e4f

Magnuson, J., S. Carpenter, and E. Stanley. 2020*a*. North temperate lakes LTER: Physical limnology of primary study lakes 1981–Current ver 27. Environmental Data Initiative.

Magnuson, J., S. Carpenter, and E. Stanley. 2020*b*. North temperate lakes LTER: Chlorophyll—Trout Lake Area 1981—Current ver 30. Environmental Data Initiative.

Magnuson, J., S. Carpenter, and E. Stanley. 2021*a*. North temperate lakes LTER: Secchi disk depth; other auxiliary base crew sample data 1981—Current ver 30. Environmental Data Initiative.

Magnuson, J., S. Carpenter, and E. Stanley. 2021*b*. North temperate lakes LTER Yahara Lakes district Bathymetry ver 10. Environmental Data Initiative. doi:10.6073/pasta/fe4f22972729b68f0398146e5ff396aa.

Manning, C. C., R. H. R. Stanley, D. P. Nicholson, B. Loose, A. Lovely, P. Schlosser, and B. G. Hatcher. 2019. Changes in gross oxygen production, net oxygen production, and air-water exchange during seasonal ice melt in Whycocomagh Bay, a Canadian estuary in the Bras d'Or Lake system. Biogeosciences **16**: 3351–3376. doi:10.5194/bg-16-3351-2019

Matsuzaki, S. S., R. C. Lathrop, S. R. Carpenter, J. R. Walsh, M. J. Vander Zanden, M. R. Gahler, and E. H. Stanley. 2021. Climate and food web effects on the spring clear-water phase in two north-temperate eutrophic lakes. Limnol. Oceanogr. **66**: 30–46. doi:10.1002/lno.11584

McCullough, I. M., and others. 2018. Dynamic modeling of organic carbon fates in lake ecosystems. Ecol. Model. **386**: 71–82. doi:10.1016/j.ecolmodel.2018.08.009

Mooij, W. M., and others. 2010. Challenges and opportunities for integrating lake ecosystem modelling approaches. Aquat. Ecol. **44**: 633–667. doi:10.1007/s10452-010-9339-3

Müller, B., L. D. Bryant, A. Matzinger, and A. Wüest. 2012. Hypolimnetic oxygen depletion in eutrophic lakes. Environ. Sci. Technol. **46**: 9964–9971. doi:10.1021/es301422r

Nielsen, A., K. Bolding, F. Hu, and D. Trolle. 2017. An open source QGIS-based workflow for model application and experimentation with aquatic ecosystems. Environ. Model. Softw. **95**: 358–364. doi:10.1016/j.envsoft.2017.06.032

Odum, H. T. 1956. Primary production in flowing waters. Limnol. Oceanogr. **1**: 102–117. doi:10.4319/lo.1956.1.2.0102

Oleksy, I. A., S. E. Jones, and C. T. Solomon. 2021. Hydrologic setting dictates the sensitivity of ecosystem metabolism to climate variability in lakes. Ecosystems. doi:10.1007/s10021-021-00718-5

Palmer, M. E., N. D. Yan, and K. M. Somers. 2014. Climate change drives coherent trends in physics and oxygen content in North American lakes. Clim. Change **124**: 285–299. doi:10.1007/s10584-014-1085-4

Phillips, J. S. 2020. Time-varying responses of lake metabolism to light and temperature. Limnol. Oceanogr. **65**: 652–666. doi:10.1002/lno.11333

Qin, B., G. Gao, G. Zhu, Y. Zhang, Y. Song, X. Tang, H. Xu, and J. Deng. 2013. Lake eutrophication and its ecosystem response. Chin. Sci. Bull. **58**: 961–970. doi:10.1007/s11434-012-5560-x

Read, J. S., D. P. Hamilton, I. D. Jones, K. Muraoka, L. A. Winslow, R. Kroiss, C. H. Wu, and E. Gaiser. 2011. Derivation of lake mixing and stratification indices from high-resolution lake buoy data. Environ. Model. Software **26**: 1325–1336. doi:10.1016/j.envsoft.2011.05.006

Read, J. S., and others. 2012. Lake-size dependency of wind shear and convection as controls on gas exchange. Geophys. Res. Lett. **39**: LO9405. doi:10.1029/2012GL051886

Read, J. S., and others. 2019. Process-guided deep learning predictions of Lake water temperature. Water Resour. Res. **55**: 9173–9190. doi:10.1029/2019WR024922

Read, J.S., and others. 2021, Data release: Process-based predictions of lake water temperature in the Midwest US U.S. Geological Survey Data Release doi:http://doi.org/10.5066/P9CA6XP8.

Rose, K. C., L. A. Winslow, J. S. Read, and G. J. A. Hansen. 2016. Climate-induced warming of lakes can be either amplified or suppressed by trends in water clarity. Limnol. Oceanogr. Lett. **1**: 44–53. doi:10.1002/lol2.10027

Sadro, S., J. M. Melack, and S. MacIntyre. 2011. Depth-integrated estimates of ecosystem metabolism in a high-elevation lake (Emerald Lake, Sierra Nevada, California). Limnol. Oceanogr. **56**: 1764–1780. doi:10.4319/lo.2011.56.5.1764

Saloranta, T. M., and T. Andersen. 2007. MyLake—A multi-year lake simulation model code suitable for uncertainty and sensitivity analysis simulations. Ecol. Model. **207**: 45–60. doi:10.1016/j.ecolmodel.2007.03.018

Scharfenberger, U., and others. 2019. Effects of trophic status, water level, and temperature on shallow lake metabolism and metabolic balance: A standardized pan-European mesocosm experiment. Limnol. Oceanogr. **64**: 616–631. doi:10.1002/lno.11064

Sobek, S., E. Durisch-Kaiser, R. Zurbrügg, N. Wongfun, M. Wessels, N. Pasche, and B. Wehrli. 2009. Organic carbon burial efficiency in lake sediments controlled by oxygen exposure time and sediment source. Limnol. Oceanogr. **54**: 2243–2254. doi:10.4319/lo.2009.54.6.2243

Solomon, C. T., and others. 2013. Ecosystem respiration: Drivers of daily variability and background respiration in lakes around the globe. Limnol. Oceanogr. **58**: 849–866. doi:10.4319/lo.2013.58.3.0849

Sommer, U., and others. 2012. Beyond the plankton ecology group (PEG) model: Mechanisms driving plankton succession. Annu. Rev. Ecol. Evol. Syst. **43**: 429–448. doi:10.1146/annurev-ecolsys-110411-160251

Sommer, U., Z. M. Gliwicz, W. Lampert, and A. Duncan. 1986. The PEG-model of seasonal succession of planktonic events in fresh waters. Arch. Hydrobiol. **106**: 433–471.

Staehr, P. A., D. Bade, M. C. Van de Bogert, G. R. Koch, C. Williamson, P. Hanson, J. J. Cole, and T. Kratz. 2010. Lake metabolism and the diel oxygen technique: State of the science: Guideline for lake metabolism studies. Limnol. Oceanogr. Methods **8**: 628–644. doi:10.4319/lom.2010.8.0628

Staehr, P. A., J. P. A. Christensen, R. D. Batt, and J. S. Read. 2012*a*. Ecosystem metabolism in a stratified lake. Limnol. Oceanogr. **57**: 1317–1330. doi:10.4319/lo.2012.57.5.1317

Staehr, P. A., J. M. Testa, W. M. Kemp, J. J. Cole, K. Sand-Jensen, and S. V. Smith. 2012*b*. The metabolism of aquatic ecosystems: History, applications, and future challenges. Aquat. Sci. **74**: 15–29. doi:10.1007/s00027-011-0199-2

Staehr, P. A., L. S. Brighenti, M. Honti, J. Christensen, and K. C. Rose. 2016. Global patterns of light saturation and photoinhibition of lake primary production. Inland Waters **6**: 593–607. doi:10.1080/IW-6.4.888

Stan Development Team. 2019. Stan Modeling Language Users Guide and Reference Manual version 2.28. http://mc-stan.org

Stan Development Team. 2020. RStan: The R interface to Stan. R package version 2.21.2. http://mc-stan.org

Steinsberger, T., R. Schwefel, A. Wüest, and B. Müller. 2020. Hypolimnetic oxygen depletion rates in deep lakes: Effects of trophic state and organic matter accumulation. Limnol. Oceanogr. **65**: 3128–3138. doi:10.1002/lno.11578

Stepanenko, V., I. Mammarella, A. Ojala, H. Miettinen, V. Lykosov, and T. Vesala. 2016. LAKE 2.0: A model for temperature, methane, carbon dioxide and oxygen dynamics in lakes. Geosci. Model Dev. **9. 5**: 1977–2006. doi:10.5194/gmd-9-1977-2016

Tsai, J.-W., and others. 2008. Seasonal dynamics, typhoons and the regulation of lake metabolism in a subtropical humic lake. Freshw. Biol. **53**: 1929–1941. doi:10.1111/j.1365-2427.2008.02017.x

Vachon, D., and Y. T. Prairie. 2013. The ecosystem size and shape dependence of gas transfer velocity versus wind speed relationships in lakes. Can. J. Fish. Aquat. Sci. **70**: 1757–1764. doi:10.1139/cjfas-2013-0241

Van de Bogert, M. C., S. R. Carpenter, J. J. Cole, and M. L. Pace. 2007. Assessing pelagic and benthic metabolism using free water measurements: Benthic and pelagic metabolism. Limnol. Oceanogr. Methods **5**: 145–155. doi:10.4319/lom.2007.5.145

Walter, J. A., R. Fleck, J. H. Kastens, M. L. Pace, and G. M. Wilkinson. 2020. Temporal coherence between lake and landscape primary productivity. Ecosystems **24**: 502–515. doi:10.1007/s10021-020-00531-6

Webster, K. E., T. K. Kratz, C. J. Bowser, J. J. Magnuson, and W. J. Rose. 1996. The influence of landscape position on lake chemical responses to drought in northern Wisconsin. Limnol. Oceanogr. **41**: 977–984. doi:10.4319/lo.1996.41.5.0977

Winslow, L. A., J. A. Zwart, R. D. Batt, H. A. Dugan, R. I. Woolway, J. R. Corman, P. C. Hanson, and J. S. Read. 2016. LakeMetabolizer: An R package for estimating lake metabolism from free-water oxygen using diverse statistical methods. Inland Waters **6**: 622–636. doi:10.5268/IW-6.4.883

Woolway, R. I., and others. 2021. Phenological shifts in lake stratification under climate change. Nat. Commun. **12**: 2318. doi:10.1038/s41467-021-22657-4

Xia, Y., and others. 2012. Continental-scale water and energy flux analysis and validation for the North American Land Data Assimilation System project phase 2 (NLDAS-2): 1. Intercomparison and application of model products: WATER AND ENERGY FLUX ANALYSIS. J. Geophys. Res. Atmos. **117**: D3.1–D3.27. doi:10.1029/2011JD016048

Yu, L., T. Liu, K. Bu, F. Yan, J. Yang, L. Chang, and S. Zhang. 2017. Monitoring the long term vegetation phenology change in Northeast China from 1982 to 2015. Sci. Rep. **7**: 14770. doi:10.1038/s41598-017-14918-4

Acknowledgments

The authors are very thankful to insights and comments from Samantha Oliver, Jordan Read, Imme Ebert-Uphoff, Sally MacIntyre, and Jared Willard. Adrianna Gorsky found and shared the quote from Edward Birge, which fit so well into our concept of metabolism phenology. The authors thank Charles Yackulic, Philip Savoy, and four anonymous reviewers for their time and their valuable critiques. The authors are thankful to the guidance and support from John Melack in revising and improving this manuscript. Lake data were obtained from the North Temperate Lakes Long-Term Ecological Research program (#DEB-1440297 and #DEB-2025982). The project was funded through a United States National Science Foundation (NSF) ABI development grant (#DBI 1759865), UW-Madison Data Science Initiative grant, and NSF HDR grant (#1934633). Any use of trade, firm, or product names is for descriptive purposes only and does not imply endorsement by the U.S. Government.

Conflicts of interest

None declared.

Submitted 26 April 2021
Revised 27 July 2021
Accepted 27 April 2022

Associate editor: John M. Melack